



Response of carbon and water fluxes to environmental variability in two Eastern North American forests of similar-age but contrasting leaf-retention and shape strategies

5 Eric R. Beamesderfer¹, M. Altaf Arain¹, Myroslava Khomik¹, Jason J. Brodeur¹, Brandon M. Burns¹

¹School of Geography and Earth Sciences and McMaster Centre for Climate Change, McMaster University, Hamilton, Ontario, L8S 4L8, Canada

Correspondence to: M. Altaf Arain (arainm@mcmaster.ca)

Abstract. The annual carbon and water dynamics of two Eastern North American forests were compared over a six year
10 period from 2012 to 2017. The geographic location, forest age, soil, and climate were similar between the sites, however, the species composition varied: one was a deciduous broadleaf forest, while the other an evergreen needleleaf forest. During the 6-year study period, the mean annual net ecosystem productivity (NEP) of the coniferous forest was slightly higher and more variable ($218 \pm 109 \text{ g C m}^{-2} \text{ yr}^{-1}$) compared to that of the deciduous broadleaf forest NEP of $200 \pm 83 \text{ g C m}^{-2} \text{ yr}^{-1}$. Similarly, the mean annual evapotranspiration (ET) of the conifer forest over the 6-year study period was higher ($442 \pm 33 \text{ mm yr}^{-1}$)
15 compared to that of the broadleaf forest ($388 \pm 34 \text{ mm yr}^{-1}$), but with similar interannual variability. Significant abnormalities in fluxes were measured between sites during drought years. Summer meteorology greatly impacted fluxes at both sites, but to varying degrees and with varying responses. In general, warm temperatures caused higher ecosystem respiration (RE), resulting in reduced mean annual NEP values – an impact that was more pronounced at the deciduous broadleaf forest compared to the evergreen needle-leaf forest. However, during drought years, the evergreen forest saw
20 greater annual reduction in carbon sequestration compared to the deciduous forest. In the evergreen conifer forest, variability of summer meteorology greatly controlled the forest's annual carbon sink-source strength. Annual ET at both forests was driven by changes in air temperature (T_a), with the largest annual ET measured in the warmest years in the deciduous forest. Additionally, prolonged dry periods with increased T_a , greatly reduced ET. During drought years, the carbon and water fluxes of the deciduous forest were less sensitive to changes in temperature or water availability compared to the evergreen
25 forest. If longer periods of increased temperatures and larger precipitation variability during summer months are to be expected under future climates, our findings suggest the carbon sink capacity of the deciduous forest will continue, while that of the conifer forest remains uncertain in the study region.

1 Introduction

Temperate forests play a significant role in the global carbon and water cycles, through their photosynthetic absorption of
30 CO_2 emissions, and through their evapotranspiration (ET) processes (Huntington, 2006; Houghton et al., 2007). In Eastern



North America, temperate forests are significant for future climate mitigation strategies, as they are impacted by warming and disturbance events (Bonan, 2008; Cubasch et al., 2013; Weed et al., 2013). These areas were a large source of carbon, due to land clearing for agricultural purposes, at the start of the 20th century (Bonan, 2008; Richart and Hewitt, 2008). With the rise of industrial development and movement of agriculture into western states, many of these agricultural areas were
35 abandoned and reforested through natural regrowth and afforestation practices (Canadell and Raupach, 2008). Within the mixed wood plains ecozone in the Great Lakes region of Canada and the USA, much of the current forested area is comprised of plantation or managed forests in different stages of growth (Wiken et al., 2011).

Recent increases in extreme weather, such as drought and heat stress, or the absence of winter snow or freezing events, may directly impact the abilities of forests to sequester carbon, adversely impacting regional forest-atmosphere interactions
40 (Allen et al., 2010; Teskey et al., 2015). Furthermore, forests have the ability to dampen or deepen the effects of warming, acting as climate feedback systems (Bonan, 2008). With continued extreme weather and insufficient water availability, due to more frequent intermittent drought events, carbon assimilation and ET in forests could be hindered, leading to positive feedbacks of continued warming and decreased water availability (Bréda et al., 2006; Choat et al., 2012; Wu et al., 2013). Given the uncertainty of the duration and timing of future extreme weather events, it is necessary to further improve our
45 understanding of the controls and limitations of carbon and water cycles in forests under changing climates.

The result of a shifting climate may lead to different impacts on deciduous broadleaf and evergreen needleleaf ecosystems, as regions once dominated by needle-leaved conifers may yield way to more deciduous broad-leaved species (Givnish, 2002; Bonan, 2008). Such a shift could disturb carbon and water cycles, as deciduous broadleaf forests typically experience higher rates of photosynthesis when compared to evergreen conifers. Some deciduous forests have also been
50 shown to reduce transpiration and ecosystem respiration during drought events (Givnish, 2002; Ciais et al., 2005). Conversely, evergreen conifer forests routinely experience a longer photosynthetic season than deciduous forests, albeit at lower rates (Barr et al., 2002). Even for climatically and geographically similar forests, differences in the timing of photosynthesis and respiration would lead to asymmetries in the partitioning of the resulting fluxes, as well as overall forest productivity and longevity.

While many studies have examined the annual carbon and water fluxes within specific land use and forest types, to date, only a handful of studies have compared these fluxes among similar-age deciduous broadleaf and evergreen coniferous forest stands growing in close proximity, in similar climatic and edaphic conditions (Gaumont-Guay et al., 2009; Baldocchi et al., 2010; Novick et al., 2015; Wagle et al., 2016). Even fewer studies have the ability to conduct such research over sufficiently long time scales (multiple years). Such a study would help to evaluate how differing forest types will respond to
60 meteorological forcings annually and interannually, helping to investigate the long-term impacts on carbon and water exchanges (Granier et al., 2007; Novick et al., 2015). In order to understand the benefits of deciduous broadleaf and evergreen coniferous forests to terrestrial-atmosphere gas exchange and identify the factors driving that exchange, long-term comparison studies are needed.



65 The Turkey Point Observatory in southern Ontario, Canada is located near Lake Erie Lowlands at the northernmost
extent of temperate deciduous forests in Eastern North America, just south of the Great Lakes – St. Lawrence forest ecotone
(Liu, 1990). Forests in the area contain numerous North American temperate species (e.g. white oak [*Quercus Alba*], red
maple [*Acer Rubrum*], eastern white pine [*Pinus Strobus L.*], and red pine [*Pinus Resinosa*]), many at the northern extent of
their natural climatic ranges (Richart and Hewitt, 2008; Froelich et al., 2015). Four sites make up the Observatory, three
white pine plantation forests of various ages and a mixed-wood deciduous broadleaf forest.

70 Previous carbon and water studies conducted within the conifer forests of the Turkey Point Observatory have been
reported in literature (i.e. Arain and Restrepo-Coupe, 2005; Peichl and Arain, 2007; McLaren et al., 2008; Peichl et al.,
2010a; MacKay et al., 2012; Skubel et al., 2015; Chan et al., 2018). Other studies have written about variability in carbon
and water fluxes of the deciduous broadleaf forest (Beamesderfer et al., 2019). This study examines the carbon and water
exchanges between two forests of similar ages within the Turkey Point Observatory: the 80-year old (as of 2019) managed
75 white pine plantation, and the naturally regenerated, mixed-wood, white oak-dominated forest that is roughly 90-years old.
The objectives of this study are to: (1) examine seasonal and interannual dynamics of carbon and water exchanges in the two
forests growing under similar climatic and edaphic conditions, but of differing tree species composition, (2) compare
controls on overall forest productivity between the two forests, and (3) identify the responses of the forests to meteorological
events during extreme years (heat and drought). Six years of data, collected congruently at the two forest sites, from 2012
80 through 2017, will be used in this study.

2 Methods

2.1 Study Sites

The two forests are located within 20 km of each other, situated on the northern edge of Lake Erie, near St. Williams in
Norfolk County, Ontario, Canada (Table 1). Monoculture pine plantations and mixed-wood deciduous forests cover only a
85 small fraction of the agriculturally dominated landscape of southern Ontario. The deciduous broadleaf forest (from here on
abbreviated and referred to as, Turkey Point Deciduous, TPD) was naturally regenerated in the early 1900s from abandoned
agricultural land-use on natural sandy terrain. The forest is classified as an uneven aged (70 – 110 years-old with a mean age
of roughly 90-years) oak-dominated forest. The stand is dominated by white oak (*Quercus Alba*), with secondary hardwood
species including: red maple (*Acer Rubrum*), sugar maple (*Acer Saccharum*), black oak (*Quercus Velutina*), red oak
90 (*Quercus Rubra*), white ash (*Fraxinus Americana*), yellow birch (*Betula alleghaniensis*), and American beech (*Fagus
Grandifolia*). Conifer species including make up a minor component (~5%) of the total tree population (Kula, 2014). The
understory is made up of young deciduous trees as well as Canadian mayflower (*Maianthemum canadense*), putty root
(*Aplectrum hymale*), yellow mandarin (*Disporum lanuginosum*), red trillium (*Trillium erectum*), and horsetail (*Equistum*).



95 The white pine plantation in this study, referred to as Turkey Point 39 (TP39 from here on), was planted in 1939 on
cleared oak-savanna lands. The dominant tree species in the 80-year old (as of 2019) site are white pine (*Pinus Strobus* L.)
and balsam fir (*Abies balsamifera* L. Mill), making up 82% and 11% of the tree population, respectively. The remaining 7%
of trees are typical native eastern North American forest species, which include: white oak, black oak, red maple, wild black
cherry (*Prunus serotina* Ehrh.) and white birch (*Betula papyrifera*). The understory consists of young white pines, oak,
100 balsam fir, and black cherry trees, as well as other ground vegetation, including: bracken fern (*Pteridium aquilinum*),
blackberry (*Rubus* spp.), poison ivy (*Rhus radicans*), moss (*Polytrichum* spp.), and Canada Mayflower. The conifer forest
has been managed on two occasions in the past (i.e. 1983 & 2012). In the early winter of 2012, the stand was thinned by
harvesting one third of the trees, which reduced the stand density (Table 1). We acknowledge the disturbance at the conifer
site at the beginning of our comparison period, though the objectives of this study were not to examine the impacts of this
105 disturbance.

The two forests differ in vegetation cover and canopy structure, but experience nearly identical edaphic and climatic
conditions. Both sites are located within the Southern Norfolk Sand Plains, historically defined by coarse-grained, sandy
deposits from glacial melt water (Richart and Hewitt, 2008). The soils at each forest are predominantly sandy (greater than
90% sand), classified by the Canadian Soil Classification Scheme as Brunisolic grey-brown luvisol (Present and Acton,
110 1984). They are both well-drained with a low-to-moderate water holding capacity (McLaren et al., 2008). Further soil and
site details can be found in Arain and Restrepo-Coupe (2005), Peichl et al. (2010a), and Beamesderfer et al. (2019a). The
climate of the region is humid temperate with warm, humid summers and cool winters. The moderating effect of Lake Erie
helps to control cold winter temperatures. The 30-year (from 1981 to 2010) mean annual air temperature and total
precipitation measured at the Environment Canada Delhi CDA weather station (25 km north of sites) were 8.0°C and 997
115 mm, respectively. Total precipitation is normally evenly distributed throughout the year, with 13% of that falling as snow
(Environment and Climate Change Canada). The data presented from these forest sites are readily available following the
global FluxNet and AmeriFlux initiatives, with the sites also known as CA-TPD (TPD) and CA-TP4 (TP39).

2.2 Eddy Covariance and Meteorological Measurements

Half-hourly fluxes of momentum, energy, water vapor, and CO₂ (Fc) have been measured continuously at TP39 and TPD
120 using closed-path eddy covariance (EC) systems since 2003 and 2012, respectively. This study examines the first 6 years
(2012 to 2017) of data at the deciduous forest, and the corresponding period for the conifer forest, though measurements at
both sites are still ongoing. The closed-path EC systems consist of a 3D sonic anemometer (CSAT3, Campbell Scientific
Inc.) and an infrared gas analyzer (IRGA); an LI-7000 (LI-COR Inc.) at TP39 and an LI-7200 (LI-COR Inc.) at TPD. The
specific details of the two EC systems are outlined in the supplementary Table A1. At both sites, IRGAs are calibrated
125 monthly using high purity N₂ gas for the zero offset, and Environment Canada Greenhouse gas specified CO₂ for the span.



The CO₂ storage (S_{CO_2}) in the air column below the EC sensors is calculated by vertically integrating the half-hourly difference in CO₂ concentrations. This calculation is completed for both the canopy and mid-canopy gas analyzers (Table A1). Half-hourly net ecosystem exchange (NEE, $\mu\text{mol m}^{-2} \text{s}^{-1}$) is calculated as the sum of the vertical CO₂ flux (F_c), and the rate of CO₂ storage (S_{CO_2}) change in the air column below each IRGA ($NEE = F_c + S_{CO_2}$). Horizontal and vertical advections were assumed to average to zero over long periods and were not considered. Half-hourly net ecosystem productivity (NEP) was calculated as the opposite of NEE ($NEP = -NEE$), where positive NEP ($-NEE$) indicates net carbon uptake by the forest (sink), and negative NEP ($+NEE$) is carbon loss from the forest to the atmosphere (source).

Meteorological measurements have been conducted alongside EC measurements during the entire measurement period at both sites. Air temperature (T_a), relative humidity (RH), wind speed and direction, downward and upward photosynthetically active radiation (PAR), and the four-components of radiation (R_n) are measured at the specified EC sampling heights for both sites (Table A1). Soil temperature (T_s) and soil water content (θ) are measured at 2, 5, 10, 20, 50, and 100 cm depths in two soil pit locations at both sites. At TPD, precipitation (P) is measured in a small forest opening, 350 m southwest of the tower. Precipitation data are cross-checked and gapfilled from data collected by the Environment Canada Delhi CDA weather station as well as from an accumulation rain gauge (GEONOR), installed 1 km south of TP39. This analysis will focus on P data from the accumulation rain gauge. All meteorological, soil, and P data were recorded using data loggers with automated data downloads occurring every half hour on desktop computers located at the base of the scaffold walk-up towers located at each site.

2.3 Eddy Covariance Data Processing

All meteorological and flux data were quality controlled, filtered, and cleaned (threshold and point cleaning) on lab-developed software following the FluxNet Canada Research Network (FCRN) guidelines (Brodeur, 2014). Data was frequently cross-checked with the AmeriFlux Network, before submission to publicly available datasets. Outliers in the data were identified and removed, while missing data was gapfilled. Small gaps in the data (hours) due to instrument malfunctions, power failures, or instrument calibration, were filled by linear interpolation, while larger gaps (hours to days) were filled using linear regression-model fitted values from other Turkey Point Observatory sites. Overall, the mean flux recovery was 91% (from 83% to 94%) at TPD and 88% (from 79% to 94%) at TP39 over the 6-years of data collection. The data initially recovered and quality controlled was then subject to footprint threshold and friction velocity (u^*) threshold (u^{*Th}) passing methods. For every half-hourly measurement, a footprint model (Kljun et al., 2004) was applied to exclude fluxes when greater than 10% of the flux footprint extended outside of the defined forest boundary (Brodeur, 2014). Following the footprint passing method, the remaining flux data recovery was 59% (from 54% to 64%) at TPD and 72% (from 67% to 77%) at TP39. Moreover, during periods of low turbulence, EC systems often underestimate fluxes. As a result, inaccurate measurements captured during periods of low turbulence were removed when measured u^* was below thresholds estimated using a u^{*Th} Moving Point Test determination method (Reichstein et al., 2005; Papale et al., 2006; Barr et al., 2013). A mean, site specific, u^{*Th} of 0.40 m s^{-1} (TPD) and 0.49 m s^{-1} (TP39) was calculated, where daytime and



160 nighttime NEE values with u^* below this threshold were removed. These data were filled using exponential relationships between sufficiently turbulent ($u^* > u^{*Th}$) NEE and T_s at 2 cm depth. The final mean annual flux recovery following both threshold passing methods was 49% (from 46% to 53%) at TPD and 53% (from 48% to 57%) at TP39 during the 6-years of measurements.

Gaps in ecosystem respiration (RE) were modelled similarly for both sites, as a function of $T_{s_{5cm}}$ and θ_{0-30cm} (average
165 from measurements made at 5, 10, 20, & 50 cm depths) using fitted ordinary least square non-linear regression models applied to half-hourly nighttime NEE. This was done in order to describe the relationship between RE and $T_{s_{5cm}}$, representing the diurnal variation in T_a , modified by a soil moisture (θ) function as shown (Brodeur, 2014):

$$170 \quad RE = R_{10} \times Q_{10}^{\frac{(T_{s_{5cm}} - 10)}{10}} \times \frac{1}{[1 + \exp(a_1 - a_2 \theta_{0-30cm})]}, \quad (1)$$

where R_{10} and Q_{10} are fitted temperature response parameters describing the RE and $T_{s_{5cm}}$ relationship, while a_1 and a_2 are fitted parameters ranging from 0 to 1, as a function of the independent variable, θ_{0-30cm} , acting to scale the RE relationship. Modeled daytime RE was then added to measured NEP to estimate the gross ecosystem productivity (GEP). When half-
175 hourly periods existed with gaps in NEP, GEP was modeled using a rectangular hyperbolic function:

$$GEP = \frac{\alpha PAR A_{max}}{\alpha PAn + A_{max}} \times f(T_{s_{5cm}}) \times f(VPD) \times f(\theta_{0-30cm}), \quad (2)$$

where the first term defines the relationship between PAR and GEP, through the calculation of the photosynthetic flux
180 per quanta (α , quantum yield) and the light-saturated rate of CO_2 fixation (A_{max}). The remaining terms describe sigmoidal scales (ranging from 0 to 1) responses of GEP to T_s , vapor pressure deficit (VPD), and θ_{0-30cm} , respectively. During half-hourly periods where meteorological data were missing, gaps in RE and GEP were filled using a non-linear regression approach and a marginal distribution sampling approach (Reichstein et al., 2005; Brodeur, 2014). Missing NEP data due to instrumentation errors, maintenance, calibrations, and power outages, were filled as the difference between the modeled RE
185 and modeled GEP.

These gapfilling methods were further used to explore relationships between each sites component fluxes (RE and GEP) and controlling meteorological and edaphic variables using residual analyses. RE and GEP gapfilling models (see above) were parameterized using pooled data from the phenologically-derived summer months (end of greenup to start of browndown, defined in the next section) for all years (2012 to 2017). Furthermore, much like other temperate forests, due to
190 the influence of canopy cover and optimal growing conditions, summer was identified as a key period for carbon uptake at both sites. Based on the functional models used to estimate fluxes (see above), controlling meteorological variables were separated into ‘driving’ ($T_{s_{5cm}}$ for RE; PAR for GEP) and ‘scaling’ (θ_{0-30cm} for RE; T_a , θ_{0-30cm} , VPD for GEP) variables. In this approach, the functional form for the driving variables defines a theoretical maximum flux for a given value of driving variable, while the scaling variables modify the magnitude of the flux by a normalized factor (between 0 and 1) depending



195 on its value. The influence of each ‘scaling’ variable on component fluxes was examined by removing one from the model,
re-parameterizing, and regressing the model residuals (predicted - modeled flux) as a function of the removed variable. This
approach provided a measure of the removed variable’s influence on component fluxes as a function of its magnitude. The
relationships derived using this approach were used in conjunction with the functional relationships derived during
parameterization using all available variables to characterize the nature of effects, and quantify the total effect of a given
200 variable during a particular season.

While the ultimate focus of this study was to compare differences in carbon fluxes between the two forests, the flux of
water vapor was also essential to the analysis and necessary for the calculation of key variables. Following the
aforementioned threshold and point cleaning, gaps in the latent heat flux (LE), and therefore the mass equivalent
evapotranspiration (ET), were filled using an artificial neural network which utilized net radiation (Rn), wind speed, $T_{s_{5cm}}$,
205 VPD, and θ_{0-30cm} (Brodeur, 2014). Following the approach outlined by Amiro et al. (2006), any remaining gaps in LE data
were filled using a moving window linear regression method. Past studies examining the relationships between ET and
meteorological variables for the forests of the Turkey Point Observatory have found T_a to largely drive ET, with smaller
secondary effects driven by VPD and θ_{0-30cm} during water or heat stressed periods (McLaren et al., 2008; MacKay et al.,
2012; Skubel et al., 2015; Burns, 2017).

210 Lastly, we implemented the analysis of variance (ANOVA) and multivariate analysis of variance (MANOVA) techniques
to evaluate statistical differences between groups (deciduous [TPD] versus coniferous [TP39]) on a set of dependent
variables (i.e. GEP, RE, NEP, and ET) as well as differences in slopes of environmental response functions (i.e. resource
efficiencies discussed in the next section). For all EC and meteorological data, processing and analyses were completed
using MatLab R2014b software (The MathWorks Inc.).

215 **2.4 Definitions of key climatic and plant-physiological variables**

In this study, we define the term drought similar to Wolf et al. (2013), in that drought periods are related to deficits in
precipitation, which impose either plant physiological stress due to decreased soil moisture (θ) or impose stress due to
stomatal closures in response to high VPD.

Two resource efficiencies were calculated at both forests to compare the links between productivity and resource supply
220 in order to reveal differences in their responses to changing climatic conditions. The amount of carbon fixed through
photosynthesis per unit of absorbed solar radiation, described as the photosynthetic light use efficiency (LUE) was calculated
as:

$$\text{LUE} = \frac{\text{GEP}}{\text{APAR}} \quad (3)$$

225 where GEP is equivalent to the carbon fixed through photosynthesis, and APAR is the portion of photosynthetically
active radiation (PAR) that is absorbed (Jenkins et al., 2007; Liu et al., 2019). The forest canopy radiation budget used in the
calculation of APAR is described as:



$$\text{APAR} = \text{PAR}_{\text{dn}} - \text{PAR}_{\text{up}} - \text{PAR}_{\text{ground}} \quad (4)$$

230

where PAR_{dn} is the incident PAR measured by PAR sensors mounted at the top of each tower facing skyward, PAR_{up} is measured as reflected PAR by instruments mounted at the same height as the PAR_{dn} sensor, but facing downward towards the forest canopy. $\text{PAR}_{\text{ground}}$ is the PAR transmitted through the canopy to a ground sensor located at 2 m height. Furthermore, the forest-level water-use efficiency (WUE), describing the carbon fixed through photosynthesis per water lost, was calculated as the ratio of GEP to ET (Keenan et al., 2013).

235

Using the methods of Gonsamo et al. (2013), we calculated phenologically-derived seasons for each year for each site. From half-hourly non-gapfilled data, the maximum daily photosynthetic uptake (GEP_{Max}) was calculated and fit using a double logistic function described by Gonsamo et al. (2013). From the initial fit, a Grubb's test was conducted to statistically ($p < 0.01$) remove outliers in GEP_{Max} data using the approach outlined by Gu et al. (2009). With outliers removed, the function was fit once more. This approach calculated photosynthetic transition dates, hereafter described as phenological dates, using first, second, and third derivatives of the logistics curves. The second derivatives estimated the end of greenup (EOG), the length of canopy closure (LOCC), and the start of browndown (SOB), while the third derivatives calculated the start of the growing season (SOS), and the end of the growing season (EOS). The start of the growing season (SOS) marked the end of winter dormancy and the beginning of the spring season, leaf emergence/greenup. The phenologically defined spring season is defined as the period from SOS to EOG. The phenologically defined summer or peak carbon uptake period is defined as the entire LOCC period from the final day of greenup (EOG) to the initiation of leaf senescence (SOB), bound by spring and autumn shoulder seasons. Finally, the resulting phenologically defined autumn season is from SOB date to EOS date, with EOS marking leaf abscission and the end of photosynthetic activity in autumn. The length of the overall growing season (LOS) was calculated as the number of days between SOS and EOS.

240

245

250

Lastly, the impact of climate on phenology was examined by the use of growing degree days (GDD) and cooling degree days (CDD), in order to understand the thermal response of each forest. GDD accumulation was defined to occur when the mean daily T_a was greater than 0°C , while CDD were calculated using the daily mean T_a below a base T_a of 20°C (Richardson et al., 2006; Gill et al., 2015). Cumulative GDD and CDD were briefly considered in this analysis.

3 Results

255

3.1 Meteorological Variability

Air temperature (T_a) measurements conducted above the canopies at both sites showed that the daily mean values of T_a at TP39 (Fig. 1a) and TPD (Fig. 1b) responded similarly (Fig. 1c) over the study period. All years experienced annual mean T_a greater than the 30-year mean (8.0°C). Record warm T_a conditions were measured throughout the majority of the year in 2012 and during the summer of 2016. Cooler conditions dominated 2013 and 2014, while these years had a higher magnitude of extreme cold days in winter, acting to decrease mean annual T_a . In 2015, 2016, and 2017, autumn warming

260



was observed, with record T_a outside of the normal peak summer period. Overall, T_a at both sites was almost identical (Fig. 1c), highlighting the similar climate both sites were growing in during the study period.

Meteorological conditions between the sites were further examined, beginning with the amount of photosynthetically active radiation absorbed by the forest canopy (APAR, Fig. 2a). The use of different sensors (Table A1) and corresponding coefficients needed for the calculation of incoming PAR_{dn}, likely led to some of the discrepancies in the total magnitudes of APAR. However, the shapes of annual APAR provide insight on the seasonal PAR absorbed by the canopy of each forest. At TP39, APAR was similar throughout the year due to the continuous presence of a dense canopy, with a nearly constant fraction (FPAR) of PAR_{dn} being absorbed. At TPD, APAR showed lower values in the winter seasons when the forest was leafless. The timing of the peak APAR at TPD was similar to TP39, though it varied each year based on the annual timing of canopy development. Daily reductions in PAR often coincided with cloudy conditions and precipitation (P) events (Fig. 2a).

Fewer P events were measured during the first half of 2012, and most of 2015, 2016, and the late-summer of 2017, as the latter three years had annual P less than the 30-year mean (997 mm). Autumn P in 2012 helped the forests to recover from the record heat and water deficits, while 2013 and 2014 experienced consistent rain throughout much of the year.

Heightened daily vapor pressure deficit (VPD, Fig. 2b) was experienced throughout 2012 by both sites, with seasonal maximum values measured during warm and dry conditions. In all years, except for 2012 and the autumn of 2016, daily VPD at TP39 was higher than at TPD (Fig. 2c). Annually, mean VPD was on average about 0.04 kPa higher at TP39 than TPD, with 2012 being the obvious exception (Fig. 2c).

Soil temperatures (T_s) at 5 cm soil depths followed closely to T_a (Fig. 1) with dampening effects evident at deeper (100 cm) soil layers (Fig. 2d). The differences in $T_{s_{5cm}}$ were explained by the species compositions of the two forests (Fig. 2e). At TPD, when the deciduous forest was leafless in winter and spring, $T_{s_{5cm}}$ was higher than at TP39 as the soil received more direct radiation. However, during the summer and autumn of each year, $T_{s_{5cm}}$ at TP39 exceeded that of TPD.

Lastly, the volumetric water content from 0-30 cm depths (θ_{0-30cm}) followed similar patterns between sites, with prolonged summer θ deficits in 2012, 2016, and 2017 (Fig. 2f). The magnitudes again were different, but each forest experienced similar declining θ and the subsequent recharging θ analogous to local P events. In the summer θ was typically lower at TPD than TP39, while all other times of the year TP39 was higher (Fig. 2g).

3.2 Phenological Variability

The meteorological conditions had a significant impact on the timing and duration of key phenological events, although ultimately the response was governed by different leaf-strategies of the various dominant tree species in each forest. The phenological transition dates and seasons calculated from EC-flux data are shown in Table 2 and Fig. 3. The start of the growing season (SOS) varied considerably between the two forests, with the SOS at the evergreen forest, TP39, beginning on average 38 ± 14 days earlier than at the deciduous forest, TPD. TP39 experienced a larger variation in SOS dates, spanning a period of 26 days between the earliest (10 March 2012; day 70) and latest (6 April 2014; day 96) years, while TPD varied by 11 days between years.



295 Growing degree days (GDD) are a proxy used to assess the amount of heat the ecosystem has absorbed, as a result of
increasing air temperatures. The response of the forests to changes in GDD was considered as a trigger for the SOS. The
cumulative GDD from the start of the year (January 1st, day 1) to 6-year mean day of season growth (25 March; day 84), was
found to be highly correlated to SOS at TP39 ($R^2 = 0.81$), but not at TPD (Fig. 4a & 4b). However, the cumulative heat
absorbed around the time of the start of greenup, which we calculated as GDD for days of year 117-127 (27 April to 7 May;
which represented the range of 6-year mean SOS data \pm one standard deviation) was found to significantly influence the SOS
300 at TPD ($R^2 = 0.95$), with a weaker influence at TP39 (days 73-95; $R^2 = 0.76$). This difference likely reflects the different
leaf-strategies, in that evergreen trees are ready to start photosynthesizing as soon as conditions are favorable, while the
deciduous trees still need to grow their leaves once conditions are favorable, before comparable rates of photosynthesis can
start. Spring, defined as the period from SOS to the end of greenup (EOG), was more than double the length (69 ± 14 days)
at TP39 when compared to TPD (31 ± 5 days). However, even with largely different SOS and spring lengths, the peak
305 summer period, defined as the period between the end of greenup (EOG) in spring and the start of browndown (SOB) in
autumn, was essentially identical between the forests (Fig. 3). This period, spanning June, July, and August, was found to be
a key contributor to the net annual productivity of each forest (discussed in sections further below).

With similar peak summer lengths, the forests began senescence at similar times, though the length of autumn, the period
from the SOB to the end of the growing season (EOS), varied considerably between the forests, due to differences in the
310 timing of the EOS (Fig. 3). Drought conditions in the summer of 2012 led both sites to have the shortest autumns and earliest
EOS (Fig. 2f & 3). Conversely, the late season warming in the autumns of 2016 and 2017 helped to prolong the growing
season at both sites, but the impacts of late season warming in 2015 were not as evident in shaping the timing of EOS (Fig. 1
& 3; Table 2).

Ultimately, the timing of the end of the growing season (EOS) was found to be influenced by a certain degree of cooling
315 (i.e. cooling degree days, CDD). At both sites, the cumulative CDD from days 230 to 290 (mid-August to mid-October),
were found to be highly correlated to the EOS at TP39 ($R^2 = 0.84$) and TPD ($R^2 = 0.95$) (Fig. 4e & 4f). Temperature
responses in both the spring (i.e. GDD) and autumn (i.e. CDD) were much higher for TPD than TP39 (Fig. 4), likely due to
the deciduous nature of the forest. These results suggest that warmer winter and early spring (i.e. January to April)
conditions will lead to an advancement of the SOS in the conifer forest, but the same cannot be said for the deciduous forest,
320 whose SOS dates were heavily dependent on late-April, early-May growing conditions. To a certain degree, both forests
responded similarly in autumn, however physiological constraints of the different tree leaf-strategies defined the overall
differences in growing season lengths.

3.3 Carbon and Water Fluxes

The water (evapotranspiration) and carbon (photosynthesis and respiration) fluxes were analyzed in both forests from 2012
325 to 2017, with the daily patterns of these fluxes illustrated in Fig. 3 and expanded upon in Table 3. At first glance, each forest
responded similarly between years, but significant seasonal irregularities existed, governing annual fluxes.



Annual photosynthesis (GEP) within the conifer forest (TP39) was the highest in 2017 (1709 g C m² yr⁻¹) and 2015 (1701 g C m² yr⁻¹), while the lowest annual GEP was measured in 2012 (1452 g C m² yr⁻¹) and 2013 (1501 g C m² yr⁻¹). GEP reductions during these years were due to opposing influences, with 2012 experiencing heat and drought conditions for most of the year, and 2013 experiencing cooler Ta and the highest annual P (1266 mm), reducing PAR and therefore GEP (Fig. 3a). At the deciduous forest (TPD), similar GEP reductions were captured in 2012 (1198 g C m² yr⁻¹), but not in 2013 (1369 g C m² yr⁻¹) due to high photosynthetic gains, outside of the 2013 peak growing season (i.e. in the early spring and autumn periods). The highest annual GEP at TPD was found in 2016 (1420 g C m² yr⁻¹) and 2017 (1447 g C m² yr⁻¹) due to warm summer conditions (Fig. 3b). Although 2014 had one of the shortest summers and the shortest overall growing season length of all years, high daily GEP rates were sustained through the summer, resulting in the year having above average annual GEP (1382 g C m² yr⁻¹). In all 6-years, spring was the only season when daily GEP was similar between the forests, as the advancement of SOS at TP39 did not greatly benefit the forest due to prevailing meteorological conditions (i.e. low PAR, Ta, etc.). However, summer and autumn daily GEP was higher at TPD when compared to TP39 across the 6-years (p < 0.01). Within individual years, the 2016 summer was the only period where seasonal GEP at TPD was sufficiently greater than at TP39 (p < 0.01). In all years, TP39 annual GEP was greater than TPD because of longer growing season lengths.

Ecosystem respiration (RE) of the conifer forest was highly variable in all years, with significant daily minimums and maximums measured throughout each summer (Fig. 3a). At TP39, the greatest annual total RE was measured in 2016 (1492 g C m² yr⁻¹) and 2017 (1525 g C m² yr⁻¹). The annual RE during these years was about 100 to 200 g C m² yr⁻¹ greater than during the other years. Cooler spring Ta and reductions in RE during the summer of 2013, led the year to have the lowest annual RE (1282 g C m² yr⁻¹) of the 6-years. While 2012 encountered reduced ET and GEP during the summer, RE was largely unaffected, leading the year to have the third highest annual RE (1386 g C m² yr⁻¹). Conversely, the 2012 RE within the deciduous forest was greatly reduced, leading to an apparent outlier in annual RE at that site (954 g C m² yr⁻¹). Similar to TP39, but to a lesser degree, the annual RE at TPD during 2017 was the greatest of the 6-years (1317 g C m² yr⁻¹). Annually, the RE at both forests responded similarly, with 2012 being the exception (Fig. 3b). The highest daily rates of RE at both sites were measured during the summer of 2013, coinciding with similar maximums in ET. In both cases, maximum rates of RE and ET occurred between precipitation events, as the soil was sufficiently wet and Ta was the highest. In all years, the spring and autumn RE was higher at TPD (p < 0.01), resulting from shorter spring and autumn periods at the deciduous forest. The summer RE though was higher at TP39 in all years and when comparing individual years, with 2013 and 2015 being the exceptions. In these years, the RE at both sites was comparable, shaping the resulting seasonal and annual differences between the two sites.

The resulting balance between photosynthesis (GEP) and ecosystem respiration (RE), net ecosystem productivity (NEP), was found to be largely irregular between sites during individual years due to site-specific differences in the timing, magnitude, and duration of daily fluctuations in GEP and RE. The trajectory of growing season NEP was strikingly different between sites (Fig. 3a & 3b). TPD (deciduous) captured consistently positive daily NEP (sink), while TP39 (conifer) was highly variable, with negative daily NEP (source) often occurring throughout the growing season. The NEP in the conifer



forest was the lowest in 2012 ($76 \text{ g C m}^{-2} \text{ yr}^{-1}$) and 2016 ($139 \text{ g C m}^{-2} \text{ yr}^{-1}$), coinciding with heat and drought stress in both years (Fig. 5a). At TP39, July 2012 was the only month during the 6-years of measurements where the peak summer growing season monthly NEP for either site was negative (source). The most productive years (largest annual source) at the conifer site were 2015 ($395 \text{ g C m}^{-2} \text{ yr}^{-1}$) and 2014 ($263 \text{ g C m}^{-2} \text{ yr}^{-1}$). While 2014 ($305 \text{ g C m}^{-2} \text{ yr}^{-1}$) was simultaneously the most productive year at the deciduous forest, 2015 ($90 \text{ g C m}^{-2} \text{ yr}^{-1}$) was the lowest annual sink, highlighting the differences between sites (Fig. 5b). Similarly, the least productive year at TP39 (2012) was the second most productive year at TPD ($292 \text{ g C m}^{-2} \text{ yr}^{-1}$). The cumulative site differences in NEP were analyzed to focus on seasonal differences (Fig. 5c). With earlier SOS at TP39, the conifer site quickly became a sink in spring, while the growing season had not yet begun at TPD. In all years except 2015, the NEP at TPD following the SOS exceeded TP39 ($p < 0.01$). In the autumn, there was no statistical difference between sites, although as photosynthesis ceased at TPD with leaf abscission, the cumulative difference in NEP between sites benefited the extended photosynthesis measured at TP39 (Fig. 5c).

Within the evergreen conifer forest (TP39), annual evapotranspiration (ET) was the highest in 2012 (495 mm yr^{-1}) and 2013 (468 mm yr^{-1}). Warm T_a throughout much of the year and high summer VPD caused 2012 to have the highest annual ET, while continuous spring and summer P (Fig. 2a) allowed 2013 to sustain higher daily rates of ET (Fig. 3a). Cooler T_a during all of 2014 (421 mm yr^{-1}) and cooler T_a in the phenological spring of 2016 (409 mm yr^{-1}), combined with the lowest annual P (in 2016), caused these years to have the lowest ET for the conifer forest (Table 3). Within the deciduous forest (TPD), 2012 (428 mm yr^{-1}), 2016 (417 mm yr^{-1}), and 2017 (403 mm yr^{-1}), had the greatest annual ET, coinciding with the years with the highest annual T_a (Fig. 1b). In 2014, the coolest year during the 6-years of measurements, annual ET (350 mm yr^{-1}) was greatly reduced at TPD. While the ET of each forest ultimately responded differently to the local meteorological forcings, on a few occasions, similar daily ET rates were measured, coinciding with significant P events. In the summer of 2013 (May 30 to July 19 or days 150 to 200), high daily ET was measured at both sites, immediately following multiple daily P events exceeding 40 mm of rain (Fig. 2a, 4a & 4b). Additionally, in 2015 (June 20 to July 10 or days 180 to 200), increased ET was measured at both sites following steady P events. Considering the 6-years as a whole, phenological autumn was the only season where ET significantly differed between the sites. While the mean autumn ET was greater at TP39, the shorter duration of autumn (Table 2) led rates of daily ET to be higher at TPD as compared to TP39 ($p < 0.01$). In this case, the phenological autumn at TPD occurred when T_a remained high, while at TP39 autumn stretched later into the year when T_a and daily ET were reduced. Both forests experienced similar annual deviations in ET (± 33 & 34 mm), and in all years except for 2016, the ET of the conifer forest exceeded that of the deciduous forest.

3.4 Forest Light and Water Use Efficiencies

The specific forest resource efficiencies (i.e. water use efficiency [WUE] & light use efficiency [LUE]) were examined to understand the relationships between forest carbon uptake and site resources (i.e. water & light), illustrated in Fig. 6. Each year, WUE varied between sites due to different forest responses to meteorological controls driving overall GEP and ET. At TP39, WUE was the highest in the spring of 2016, the summers of 2014 and 2017, autumns of 2015, 2016, and 2017 (Fig.



6a). In 2016, the SOS began early (March 15; day 74) promoting prompt increases in spring GEP, when Ta and ET remained
395 low. In autumn, the years with extended growing seasons, saw GEP increase later in the year as ET decreased, leading to
higher forest WUE. At TPD, WUE was lowest in the warm years (i.e. 2012, 2016, & 2017) due to increased annual ET,
while the cool and highly productive year of 2014 experienced the highest summer and autumn WUE (Fig. 6b). In the 6-
years of measurements, highly significant ($p < 0.01$) linear relationships of the ratio of monthly ET and GEP (calculating
WUE) were measured at both sites, with monthly WUE remaining relatively constant (Fig. 6c; $R^2 = 0.92$). While monthly
400 WUE was similar between forests (Fig. 6c), WUE was higher at TPD ($4.70 \text{ g C kg}^{-1} \text{ H}_2\text{O}$) when compared to that of TP39
($4.70 \text{ g C kg}^{-1} \text{ H}_2\text{O}$).

Even though the sites measured differences in the magnitude of APAR (Fig. 2a), the general light use efficiency (LUE)
trends and deviations were comparable. At both sites, 2014 and 2017 had the highest summer LUE, while reduced GEP at
both sites during the summers of 2012 and 2016 yielded the lowest summer LUE (Fig. 6d & 6e). Across all years, the
405 monthly linear relationships between GEP and APAR yielded similar results, with larger variation ($R^2 = 0.70$) and lower
LUE at TP39 when compared to TPD (Fig. 6f; $R^2 = 0.96$). Similarly, TPD had higher annual and summer LUE ($p < 0.01$)
resulting from greater GEP although spring and autumn LUE was similar at both sites.

3.5 Meteorological Controls on Fluxes

To better understand and the water and carbon fluxes within each forest ecosystem, the roles of various meteorological
410 variables (i.e. Ta, PAR, θ , etc.) were analysed during the study period. When first considering annual values, ET at the
deciduous (TPD) forest was found to be highly correlated ($R^2 = 0.84$) to annual mean Ta. A smaller secondary effect on ET
($R^2 = 0.83$; Table 4) was found for winter and early spring (January 1st to SOS) $\theta_{0-30\text{cm}}$, which helped to explain the impact of
winter soil water storage and seasonal water availability at the start of each year. At TPD, higher winter $\theta_{0-30\text{cm}}$ was measured
in the years with the greatest annual ET. At the conifer (TP39) forest, no strong relationships were found between annual ET
415 values and seasonal or annual meteorological variables. However, monthly linear relationships of Ta and VPD to ET were
significant at both sites (Fig. 7). The evergreen conifer and deciduous broadleaf forests experienced similar increases in
monthly ET, with increasing monthly mean Ta (Fig. 7a). While the evergreen forest saw higher ET rates compared to the
deciduous forest, the correlation of ET to Ta was greater for the deciduous forest ($R^2 = 0.95$ vs $R^2 = 0.89$; for TPD and TP39,
respectively). Similar responses between monthly ET and monthly VPD were measured, although the difference between the
420 sites was much smaller, as a mean monthly VPD of 1kPa corresponded to a monthly total ET of 104 mm and 97 mm at TP39
and TPD, respectively (Fig. 7b). Overall, the correlation of ET to increasing VPD was greater for the evergreen forest ($R^2 =$
 0.82 vs $R^2 = 0.74$; for TPD and TP39, respectively).

Following similar annual time scales used in the ET comparison, photosynthesis (GEP), respiration (RE), and net
ecosystem productivity (NEP) were compared to meteorological measurements for each site and season (Table 4). In both
425 forests, no significant relationships were found between meteorological variables and annual GEP. In terms of RE at TP39,
the years with the highest annual RE (i.e. 2016 & 2017) resulted from summer drought conditions, as evident through



prolonged reductions in mean summer $\theta_{0-30\text{cm}}$ ($R^2 = 0.89$). The years with the lowest annual RE (i.e. 2013 & 2015) were ultimately the most productive (largest annual carbon sink) and both measured the highest mean summer $\theta_{0-30\text{cm}}$. The annual NEP was correlated to the length of spring ($R^2 = 0.75$), the mean summer T_a ($R^2 = 0.73$), and most importantly, summer
430 NEP ($R^2 = 0.99$). For the evergreen conifer site, a shorter phenologic spring period due to rapid photosynthetic development was seen in years with the highest annual NEP. Higher summer T_a decreased annual NEP, highlighting the influence of limitations due to heat stress. Lastly, summer NEP at TP39 was nearly identical to the annual NEP, stressing the importance of this period (roughly June, July & August) in shaping the annual carbon sink status of the forest.

At the deciduous forest, the relationship between RE and spring T_a ($R^2 = 0.77$) suggested that warmer springs generally
435 acted to decrease annual RE. Annual NEP at the conifer forest was shown to be correlated to summer RE ($R^2 = 0.80$; Table 4). Within the deciduous forest, the years with lower summer RE (i.e. 2012, 2014) were the largest annual carbon sinks. Lastly, the smallest annual NEP (2015) was observed when summer RE was highest (714 g C m^{-2}). Ultimately, on annual time scales, both sites emphasized the importance of summer meteorological conditions on annual productivity.

Based on the importance of summer outlined above, the flux parameterizations were further examined to understand the
440 dominant meteorological factors during each summer. At the deciduous broadleaf forest, $\theta_{0-30\text{cm}}$ was shown to have no impact on GEP, while T_a , VPD, and PAR contributed to the summer photosynthesis each year (Table 5). Based on meteorological conditions experienced in each year, 2016 and 2014 were the most favorable for summer GEP, while 2012 was the least favorable. Similar results were found for the evergreen conifer forest, though at that site, low $\theta_{0-30\text{cm}}$ was shown to influence GEP. Therefore, years with lower $\theta_{0-30\text{cm}}$ or higher VPD did not experience the same beneficial meteorological inputs
445 necessary for optimal summer GEP. Outside of $T_{s_{5\text{cm}}}$, $\theta_{0-30\text{cm}}$ impacted summer RE at both sites. At TPD, the years with the highest summer $\theta_{0-30\text{cm}}$ (i.e. 2013 & 2015) experienced optimal conditions for enhanced RE, while 2012 and 2016 saw less favorable RE. Similar responses were also found at TP39. Overall, the annual fluxes were a product of the season length and predicted daily rate that were in turn influenced by variability in meteorological variables.

4 Discussion

450 4.1 Meteorological and Phenological Variability

The meteorological conditions experienced by both sites during the study period were similar and typical of temperate North American ecosystems, characterized by four distinct seasons, with cold winters and warm summers. The close proximity between the two forests (~20 km apart at the same latitude) led them to experience similar synoptic scale weather conditions during each year, and therefore nearly identical air temperature (T_a). Even with similar climatic forcings (i.e. T_a) seasonal
455 deviations in 5 cm soil temperature ($T_{s_{5\text{cm}}}$) were found, suggesting certain differences were primarily influenced by forest canopy characteristics (Palmroth et al., 2005; Stoy et al., 2006). In this case, soil temperature was linked to the proportion of incoming radiation penetrating the forest canopy, reaching the forest floor. In all years, $T_{s_{5\text{cm}}}$ at the conifer forest was higher during each summer, but lower than that of the deciduous forest during the rest of the year. In the conifer forest, branches



and needles were highly clumped while the canopy remained relatively open, leading to minor annual variations in incoming
460 radiation absorbed (APAR) by the forest canopy and soil, in line with Brummer et al. (2012). In the deciduous forest, $T_{s_{5cm}}$
was higher when leaves were absent and incoming radiation was directly absorbed by the soil. Following the development
and closure of the forest canopy in spring, deciduous $T_{s_{5cm}}$ was lower than the conifer forest in our study, which was in line
with other similar studies (i.e. Lee et al., 2010; Augusto et al., 2015).

In general, both forests had similar trends VPD in all years and TP39 had somewhat higher VPD compared to TPD,
465 except in the record warm year of 2012. The higher VPD at the deciduous forest in 2012 could be due to the relative
unresponsiveness of stomata to higher VPD typical of broadleaved species, or the suggested larger leaf boundary layers in
deciduous trees, where VPD measured above a canopy can be greater than what leaves experience (Kelliher et al., 1993;
Baldocchi and Vogel, 1996; Baldocchi et al., 2002; Stokes et al., 2006). Ultimately, minor meteorological variations between
the forests led to similar forcings during the study period, though species specific responses shaped the timing of
470 phenological events in each forest.

The response of leaf phenology in temperate forests to changes in temperature has been shown throughout much of the
Northern Hemisphere (Jeong et al., 2011; Settele et al., 2014). In future climates, rising T_a is predicted to lead to an earlier
start, later end, and prolonged duration of the growing season, though ecosystem-level responses are expected to vary as
there is a strong genetic control among plant species on the timing of phenological events (Vitasse et al., 2011; Sanz-Perez et
475 al., 2009; Polgar and Primack, 2011; Oishi et al., 2018). In locations such as ours where different tree species face similar
climates, the relative advantage of conifer species is seen as the start of the growing season (SOS) may often precede spring
frost events (Givnish, 2002; Augusto et al., 2015). On the other hand, deciduous species (such as *Quercus*) often delay leaf-
out to decrease the probability of frost damage (Kramer, 2010; Polgar and Primack, 2011), which was seen at our sites. The
mean SOS for our conifer (*Pinus Strobus* L.) forest began over a month (38 days) earlier than the deciduous (*Quercus Alba*)
480 forest, with much greater variability seen in the conifer forest especially in years with warm spring conditions. The timing of
the deciduous SOS (2 May; day 122 ± 5 days) was consistent with similar North American deciduous forests; such as
Harvard Forest (4 May; day 124 ± 14 days; in Gonsamo et al., 2015) and Morgan Monroe Forest (28 April; day 118 ± 4
days; in Dragoni et al., 2011).

In the autumn, the onset of senescence and end of the growing season (EOS) has been reported to be advanced by high
485 soil moisture (θ) deficits, and delayed with increased warming (Kramer, 2010, Warren et al., 2011; Liu et al., 2016). The
relationship between summer θ deficits and the timing of senescence were insignificant at the conifer forest, although both
forests experienced later senescence dates with decreased θ (although likely due to increased T_a), opposite to previous
studies. For the conifer forest, the two years (i.e. 2012 & 2016) with continued heat and drought stress saw the latest dates of
senescence, while at the deciduous forest, greater mean summer θ led to earlier senescence in all years but decreased θ
490 extended senescence. Instead, we found that the late-summer (August to October) degree of cooling had a significant impact
on the EOS as well as overall growing season length. This response has been confirmed by long term observational data,
which has shown strong positive correlations between T_a and EOS, helping to postpone EOS for many forest ecosystems



(Ibanez et al., 2010; Dragoni and Rahman, 2012; Gallinat et al., 2015; Liu et al., 2016). More cold days promoted earlier EOS and shorter seasons, while less cooling (greater warming) extended the season and phenologic autumn period at both sites. However, the degree of extension was much different between sites, similar to the response in spring. The mean EOS (10 November; day 314 ± 8 days) in the deciduous site occurred a month (31 days) before that of the evergreen coniferous site (11 December; day 345 ± 17 days). There was much greater variability in EOS experienced at the conifer forest compared to the deciduous broadleaf forest. Based on these findings, in future climates, evergreen conifer forests in the region may expect earlier springs, later autumns, and longer growing seasons, while the deciduous broadleaf forests will likely see greater gains in growing season length from prolonged autumns, only limited by their specific leaf-strategy.

4.2 Meteorological Impacts on Carbon Fluxes

Changes in local meteorology (and climate) have been recognized as a primary factor driving the interannual variability of carbon fluxes within forests (Bonan, 2008; Desai, 2010; Coursolle et al., 2012). T_a anomalies and seasonal fluctuations in water availability (θ) over a predictable course of the year were shown to strongly determine the carbon sequestered in many forests (Ciais et al., 2005; Sun et al., 2011; Xie et al., 2014). Conceptually, higher T_a will promote longer growing seasons and greater photosynthesis (GEP), though drawbacks due to increased respiration (RE) are expected (White and Nemani, 2003; Noormets et al., 2015). In this study, the differing forests responses to meteorological conditions led to significant divergences in annual GEP, RE, and NEP. At both sites, the overall growing season length in 2012 was the second shortest (behind 2014), despite record T_a experienced throughout much of the year. If this year is excluded, both the conifer and deciduous forests experienced longer growing season lengths with increased annual T_a . Annual GEP reductions were also experienced in each forest during the heat and drought year of 2012. GEP reductions at our conifer site may also be associated with the reduction in canopy size, due to thinning performed at the site in the early winter of 2012 (see more discussion in the following section). Additionally, higher T_a and low θ acted to enhance RE in the conifer forest, but significantly reduced RE in the deciduous forest. The suppression of RE has been previously reported for other deciduous forests during warm and dry periods (Davidson et al., 1998; Palmroth et al., 2005; Novick et al., 2015; Darenova and Cater, 2018). Overall, these reductions in both the growing season length and the magnitude of carbon fluxes highlighted the forests sensitivities to heat and drought events, though it ultimately varied between sites. Contrasting studies have shown varying results on the overall drought tolerance of conifer forests. Some studies suggest that conifer species, especially those in resource-poor locations, may be less responsive to seasonal climate anomalies (Aerts et al., 1995; Way and Oren, 2010; Wolf et al., 2013). Others have found that conifer (i.e. *Pinus*) forests are highly coupled to atmospheric demand and drought sensitivities (Griffis et al., 2003; Stoy et al., 2006). The two years (i.e. 2012 & 2016) with the lowest annual carbon sequestration (NEP) in our conifer forest were found during hot and dry years with high atmospheric demand (i.e. high VPD). These years measured the lowest summer light use efficiency (LUE, due to decreased GEP) and the lowest summer NEP, consistent with past studies (Griffis et al., 2003; Vargas et al., 2013). Similar LUE reductions were measured at the deciduous forest during the summers of 2012 and 2016, though annual NEP was drastically different due to comparable



decreases in summer and annual RE, not experienced in the conifer forest. Instead, the two drought years were some of the largest annual carbon sinks (greater positive NEP) during the six years of measurements at the deciduous forest. Similar to this study, other research has shown deciduous oak (*Quercus*) forests to be more resilient to drought than their conifer counterparts (Elliot et al., 2015; Wang et al., 2016). Studies have suggested that warm (drought) conditions may lead to
530 reduced carbon uptake or even carbon release (White and Nemani, 2003; Grant et al., 2009; Vargas et al., 2013). Based on our findings, reductions in NEP during expected future intermittent drought conditions in the area could be projected in the evergreen conifer forest, but not in the deciduous broadleaf forest.

Over the measurement period, both forests experienced similar interannual variability in all carbon fluxes ($\sim 100 \text{ g C m}^{-2} \text{ yr}^{-1}$) to that expected in midlatitude forests (Yuan et al., 2009; Desai 2010). In all years the magnitude of GEP and RE were
535 greater in the conifer forest, however, analogous increases at the deciduous forest led the two forests to have very similar annual NEP. While evergreen conifer forests have been shown to have lower photosynthetic capacities than deciduous broadleaf forests (Reich et al., 1995; Baldocchi et al., 2010), the longer growing seasons led the conifer forest in this study to have a greater magnitude of annual NEP in most years, with drought years being the exceptions. Even in drought years, both the conifer forest and the deciduous forest in our study experienced annual NEP similar to past studies conducted in the
540 temperate region of North America (Barford et al., 2001; Arain and Restrepo-Coupe, 2005; Gough et al., 2013; Xie et al., 2014; Dymond et al., 2016; Oishi et al., 2018). In the coolest year of this study (i.e. 2014), which was closest to the 30-year norm for the area in terms of its mean annual T_a , the two forests experienced similar seasonal and annual carbon uptake and some of the highest rates over the 6-year study. This suggests that both forests (especially the deciduous forest), favor meteorologically “normal” years, similar to the conclusion of Griffis et al. (2003) and Gonsamo et al. (2015). Therefore,
545 under future climates that are predicted to be warmer compared to the current 30-year norm for the area, the carbon sequestration capacity of both forests may be reduced.

4.3 Meteorological Impacts on Water Fluxes

The annual carbon uptake measured within each forest would not be possible without the availability and use of water (Baldocchi et al., 2001). With insufficient water availability annual tree growth and productivity may be limited (Nemani et
550 al., 2003; Augusto et al., 2015). Hence, it is important to understand the efficiency of water use (WUE) and the corresponding release of water vapor (evapotranspiration, ET) to the atmosphere on seasonal and annual time scales. On average, our conifer forest had greater annual ET and less variability than the deciduous forest. However, we found conflicting results between sites in regards to annual ET during drought years. At both sites, ET was shown to be strongly driven by air temperature (T_a). ET in 2012 was the highest of all years following amplified T_a for most of the year. Much
555 like RE, ET responds year-round, so warmer spring or autumn periods often lead to annual increases in ET (Schwartz et al., 2006; Taylor et al., 2008).

Similarly, in the deciduous forest, annual ET was heightened during the hot and dry year of 2016. The characteristic amplification of both T_a and VPD during warm drought years led the years with the lowest mean summer $\theta_{0-30\text{cm}}$ and highest



560 summer T_a (or VPD) to experience increased annual ET at the deciduous forest. An opposing ET response was measured in
the coniferous forest, as 2016 had the lowest annual ET, the only year where the annual conifer ET was lower than that of
the deciduous forest ET.

Typically, transpiration is beneficial to plants, helping to cool leaves and thereby reducing respiration (Rambal et al.,
2003; Baldocchi et al., 2010; Brummer et al., 2012). In our case, high summer T_a , the lowest $\theta_{0-30\text{cm}}$, and very little summer
and annual P removed most of the water from the system, significantly reducing ET, while RE continued to rise. At the
565 conifer forest, the timing of summer P appeared to greatly influence ET (i.e. 2013), as the availability of rainfall during the
physiological summer led to the greatest demand for water. Ultimately, it is likely that the differing response between sites
was due to the ability of each forest to access deep soil water. Studies have shown oak (*Quercus*) forests to be less sensitive
and more resilient to drought, due to more efficient access to deeper soil water, than conifer forests (Breda et al., 2006;
Bonan et al., 2008; Wang et al., 2016; Matheny et al., 2017). Evergreen conifer forests may have roots extending just as deep
570 as deciduous broadleaf forests, but they are not as effective at obtaining water as broadleaf trees (Oren and Pataki, 2001).
With higher atmospheric demand during dry periods often leading to greater ET across many forest types (Meinzer et al.,
2013; Wu et al., 2013; Tang et al., 2014), the access and availability of water in deep soil layers allowed the deciduous forest
to sustain high ET, even in drought years.

We found annual WUE of both forests to respond similarly across all years, though variations in GEP and ET between
575 the forests led to seasonal WUE differences due to the aforementioned responses of both fluxes. The WUE at the conifer
forest was consistent with previously reported values for that location (Brummer et al., 2012; Skubel et al., 2015), while the
deciduous forest WUE was found to be higher than an oak forest in Ohio (Xie et al., 2016). Assuming similar carbon
assimilation, this implies a higher evapotranspiration flux at the conifer forest (Augusto et al., 2015), which we saw.

4.4 Forest Management and Future Climate Impacts

580 Forest age, management practices, and historical land-use have been shown to impact annual carbon fluxes within forests
(Wofsy et al., 1993; Song and Woodcock, 2003). While our forests are of relatively similar age (~80-90 years), they have
experienced different management practices over their lifetime so far, with the conifer forest being a planted forest that
underwent low density partial thinning in 1983 and 2012, while the deciduous broadleaf forest was naturally regenerated
with nearby periodic selective harvesting in the past. The difference in carbon uptake over the forest's life will be influenced
585 by management treatments (Herbst et al., 2015). Some studies (Zha et al., 2009; Dore et al., 2012; Skubel et al., 2017) have
suggested that overall forest carbon and water fluxes recover rapidly post-disturbance. Furthermore, some studies have found
a positive correlation between species number and productivity in temperate forests (Morin et al., 2011). Similarly, mixed
forests are generally assumed to be more resilient to extreme weather events and disturbance events than mono-specific
forest stands (Pretzsch, 2014; Herbst et al., 2015). With a greater number of species in our deciduous broadleaf forest (500+
590 tree & plant species, as per Elliot et al., 1999), and the resistance to heat and drought induced carbon losses shown in this
study, it is likely that the deciduous broadleaf forests will remain a carbon sink well into the future. Even following increased



RE losses expected with warmer late-summer and autumn conditions (Dunn et al., 2007; Piao et al., 2008), such as those experienced in 2016 and 2017 at our site, the conclusions remain the same.

For similar forest types, the annual responses of GEP and RE to local meteorology will affect natural and managed forests similarly, however it has been proposed that many managed forests may already be maximized for a given T_a regime, leaving less room for adaptability or acclimation in the future (Litton and Giardina, 2008; Chen et al., 2014; Noormets et al., 2015). With RE shown to be higher in managed forests compared to natural forests (Arain and Restrepo-Coupe, 2005), it is possible that our conifer forest may see limitations in the annual carbon sequestration capability in the future. With considerable daily RE losses experienced following summer precipitation events (i.e. 2013 & 2014), enough hot periods with intermittent heavy rains in the future could cause forest RE to exceed in the conifer forest. As the climate continues to change, the management practices and responses to meteorological conditions will determine the relative carbon sink or source strength in many temperate forests.

5 Conclusions

The annual carbon and water dynamics were compared between two forests of different leaf-strategy in the Great Lakes region of southern Ontario, Canada, over a six year period from 2012 to 2017. The geographic location, forest age, soil, and climate were similar between sites, but one was an evergreen needle-leaf monoculture plantation, while the other was a mixed-wood deciduous broadleaf naturally regenerated forest. On average, the evergreen conifer forest was a greater carbon sink ($218 \pm 109 \text{ g C m}^{-2} \text{ yr}^{-1}$) with higher annual ET ($442 \pm 33 \text{ mm yr}^{-1}$) than the deciduous broadleaf forest ($200 \pm 83 \text{ g C m}^{-2} \text{ yr}^{-1}$ & $388 \pm 34 \text{ mm yr}^{-1}$, respectively). While mean annual fluxes were similar in magnitude and variation, significant abnormalities were measured between sites, especially during drought years. Summer meteorology was shown to greatly impact fluxes at both sites, though to varying degrees with varying responses. Annual NEP was reduced at the deciduous forest during years with increased summer RE. Similarly, annual deciduous forest ET was driven by changes in T_a , with the largest annual ET measured in the warmest years. During droughts, the carbon and water fluxes of the deciduous forest were less sensitive to changes in temperature or water availability. Conversely, annual NEP at the conifer forest was the result of competing influences of both GEP and RE, though ultimately, summer NEP determined annual NEP. The significant response of the conifer forest to heat and drought events led the summer months in all years to greatly control the forests annual carbon sink-source status. Additionally, prolonged dry periods with increased T_a were shown to greatly reduce ET (i.e. 2016). Both sites saw average ET, but increased NEP during ‘normal’ years, but only the conifer forest saw annual reductions in carbon sequestration during drought years. If longer summer periods of increased temperatures and larger variability in precipitation are to be expected in future climates, these findings suggest that the deciduous forest will continue to be a net carbon sink, while the response of the conifer forest remains uncertain. Given our findings, drought-induced RE increases or GEP decreases may hurt the conifer carbon uptake.



625 *Data availability.* The data presented in this study are available at: <http://dx.doi.org/10.17190/AMF/1246152> (deciduous forest) and <http://dx.doi.org/10.17190/AMF/1246012> (coniferous forest).

Author contributions. ERB collected, cleaned, and processed the data with help from JJB and BMB. ERB, MAA, and MK designed the experiment, with grants received by MAA. ERB and JJB performed the statistical analyses. ERB interpreted the
630 data, prepared the figures, and wrote the manuscript with editorial contributions from all authors.

Competing interests. The authors declare no competing interests.

Acknowledgements. This study was funded by the Natural Sciences and Engineering Research Council (NSREC), the Global
635 Water Futures Program (GWF), and the Ontario Ministry of Environment, Conservation and Parks (MOECP). Funding from the Canadian Foundation of Innovation (CFI) through New Opportunity and Leaders Opportunity Fund and Ontario Research Fund of the Ministry of Research and Innovation is also acknowledged. In kind support from the Ontario Ministry of Natural Resources and Forestry (OMNRF). The St. Williams Conservation Reserve Community Council and the Long Point Region Conservation Authority (LPRCA) are also acknowledged. We acknowledge support from Zoran Nestic at the
640 University of British Columbia in assistance with flux measurements at our site, and members of the Hydrometeorology and Climatology lab at McMaster University for their continued support at both sites.

645

650



655 References

- Abrams, Marc D.; Downs, Julie A. 1990. Successional replacement of old-growth white oak by mixed mesophytic hardwoods in southwestern Pennsylvania. *Canadian Journal of Forest Research*, 20(12), 1864-1870.
- Aerts, R., 1995. The advantages of being evergreen. *Trends Ecol. Evolut.*, 10(10), 402-407.
- Allen, C.D., Macalady, A.K., Chenchouni, H., Bachelet, D., McDowell, N., Vennetier, M., Kitzberger, T., Rigling, A.,
660 Breshears, D.D., Hogg, E.T. and Gonzalez, P., 2010. A global overview of drought and heat-induced tree mortality reveals emerging climate change risks for forests. *Forest Ecology and Management*, 259(4), 660-684.
- Amiro, B.D., Barr, A.G., Black, T.A., Iwashita, H., Kljun, N., McCaughey, J.H., Morgenstern, K., Murayama, S., Nesic, Z.,
Orchansky, A.L. and Saigusa, N., 2006. Carbon, energy and water fluxes at mature and disturbed forest sites, Saskatchewan, Canada. *Agricultural and Forest Meteorology*, 136(3-4), 237-251.
- 665 Arain, M.A., and Restrepo-Coupe, N., 2005. Net ecosystem production in a temperate pine plantation in southeastern Canada. *Agric. For. Meteorol.*, 128, 223-241.
- Augusto, L., De Schrijver, A., Vesterdal, L., Smolander, A., Prescott, C. and Ranger, J., 2015. Influences of evergreen gymnosperm and deciduous angiosperm tree species on the functioning of temperate and boreal forests. *Biological Reviews*, 90(2), 444-466.
- 670 Baldocchi, D.D. and Vogel, C.A., 1996. Energy and CO₂ flux densities above and below a temperate broad-leaved forest and a boreal pine forest. *Tree Physiology*, 16(1-2), 5-16.
- Baldocchi, D., Falge, E., Gu, L., Olson, R., Hollinger, D., Running, S., Anthoni, P., Bernhofer, C., Davis, K., Evans, R. and Fuentes, J., 2001. FLUXNET: A new tool to study the temporal and spatial variability of ecosystem-scale carbon dioxide, water vapor, and energy flux densities. *Bull. Amer. Meteor. Soc.*, 82(11), 2415-2434.
- 675 Baldocchi, D.D., Wilson, K.B. and Gu, L., 2002. How the environment, canopy structure and canopy physiological functioning influence carbon, water and energy fluxes of a temperate broad-leaved deciduous forest—an assessment with the biophysical model CANOAK. *Tree Physiology*, 22(15-16), 1065-1077.
- Baldocchi, D.D., Ma, S., Rambal, S., Misson, L., Ourcival, J.M., Limousin, J.M., Pereira, J. and Papale, D., 2010. On the differential advantages of evergreenness and deciduousness in Mediterranean oak woodlands: a flux perspective. *Ecol. Appl.*, 20(6), 1583-1597.
- 680 Barr, A.G., Griffis, T.J., Black, T.A., Lee, X., Staebler, R.M., Fuentes, J.D., Chen, Z. and Morgenstern, K., 2002. Comparing the carbon budgets of boreal and temperate deciduous forest stands. *Canadian Journal of Forest Research*, 32(5), 813-822.
- Barr, A.G., Richardson, A.D., Hollinger, D.Y., Papale, D., Arain, M.A., Bohrer, G., Dragoni, D., Fischer, M.L., Gu, L., Law, B.E., Margolis, H.A., Mccaughey, J.H., Munger, J.W., Oechel, W., Schaeffer, K., 2013. Use of change-point detection for friction-velocity threshold evaluation in eddy-covariance studies. *Ag. For. Met.*, 31-45.
- 685 Barford, C.C., Wofsy, S.C., Goulden, M.L., Munger, J.W., Pyle, E.H., Urbanski, S.P., et al., 2001. Factors controlling long- and short-term sequestration of atmospheric CO₂ in a mid-latitude forest. *Science*, 294(5547), 1688-1691.
- Beamesderfer, E.R., Arain, M.A., Khomik, M., and Brodeur, J.J., 2019. How will the carbon fluxes within the northernmost temperate deciduous forests of North America fair under future climates?. *Journal of Geophysical Research: Biogeosciences*.
- 690 Bonan, G.B., 2008. Forests and climate change: forcings, feedbacks, and the climate benefits of forests. *Science*, 320(5882), 1444-1449.
- Bréda, N., Huc, R., Granier, A., and Dreyer, E., 2006. Temperate forest trees and stands under severe drought: a review of ecophysiological responses, adaptation processes and long-term consequences. *Annals of Forest Science*, 63(6), 625-644.
- 695 Brodeur, J.J., 2014. Data-driven approaches for sustainable operation and defensible results in a long-term, multi-site ecosystem flux measurement program. McMaster University.
- Brümmer, C., Black, T.A., Jassal, R.S., Grant, N.J., Spittlehouse, D.L., Chen, B., Nesic, Z., Amiro, B.D., Arain, M.A., Barr, A.G. and Bourque, C.P.A., 2012. How climate and vegetation type influence evapotranspiration and water use efficiency in Canadian forest, peatland and grassland ecosystems. *Agricultural and Forest Meteorology*, 153, 14-30.
- 700 Burns, B., 2017. Response of Ecosystem Evapotranspiration to Water-Stress in a Temperate Deciduous Forest in southern Ontario. McMaster University.
- Canadell, J.G. and Raupach, M.R., 2008. Managing forests for climate change mitigation. *Science*, 320(5882), 1456-1457.



- 705 Chan, F.C., Arain, M.A., Khomik, M., Brodeur, J.J., Peichl, M., Restrepo-Coupe, N., Thorne, R., Beamesderfer, E.,
McKenzie, S., Xu, B. and Croft, H., 2018. Carbon, water and energy exchange dynamics of a young pine plantation
forest during the initial fourteen years of growth. *Forest Ecology and Management*, 410, 12-26.
- Chen, G., Yang, Y. and Robinson, D., 2014. Allometric constraints on, and trade-offs in, belowground carbon allocation and
their control of soil respiration across global forest ecosystems. *Global Change Biology*, 20(5), 1674-1684.
- 710 Choat, B., Jansen, S., Brodribb, T. J., Cochard, H., Delzon, S., Bhaskar, R., et al., 2012. Global convergence in the
vulnerability of forests to drought. *Nature*, 491(7426), 752-755.
- Ciais, P., Reichstein, M., Viovy, N., Granier, A., Ogee, J., Allard, V., Aubinet, M., Buchmann, N., Bernhofer, C., Carrara, A.
and Chevallier, F., 2005. Europe-wide reduction in primary productivity caused by the heat and drought in 2003. *Nature*,
437(7058), 529-533.
- 715 Coursolle, C., Margolis, H.A., Giasson, M.A., Bernier, P.Y., Amiro, B.D., Arain, M.A., Barr, A.G., Black, T.A., Goulden,
M.L., McCaughey, J.H. and Chen, J.M., 2012. Influence of stand age on the magnitude and seasonality of carbon fluxes
in Canadian forests. *Agricultural and Forest Meteorology*, 165, 136-148.
- Cubasch, U., D. Wuebbles, D. Chen, M.C. Facchini, D. Frame, N. Mahowald, and J.-G. Winther, 2013: Introduction. In:
720 *Climate Change 2013: The Physical Science Basis. Contribution of Working Group I to the Fifth Assessment Report of
the Intergovernmental Panel on Climate Change [Stocker, T.F., D. Qin, G.-K. Plattner, M. Tignor, S.K. Allen, J.
Boschung, A. Nauels, Y. Xia, V. Bex and P.M. Midgley (eds.)]. Cambridge University Press, Cambridge, United
Kingdom and New York, NY, USA.*
- Darenova, E. and Čater, M., 2018. Different structure of sessile oak stands affects soil moisture and soil CO₂ efflux. *Forest
Science*, 64(3), 340-348.
- 725 Davidson, E.A., Belk, E. and Boone, R.D., 1998. Soil water content and temperature as independent or confounded factors
controlling soil respiration in a temperate mixed hardwood forest. *Global Change Biology*, 4(2), 217-227.
- Desai, A.R., 2010. Climatic and phenological controls on coherent regional interannual variability of carbon dioxide flux in a
heterogeneous landscape. *J. Geophys. Res. G: Biogeosci.*, 115(G3).
- Dore, S., Montes-Helu, M., Hart, S.C., Hungate, B.A., Koch, G.W., Moon, J.B., Finkral, A.J. and Kolb, T.E., 2012.
730 Recovery of ponderosa pine ecosystem carbon and water fluxes from thinning and stand-replacing fire. *Global Change
Biology*, 18(10), 3171-3185.
- Dragoni, D. and Rahman, A.F., 2012. Trends in fall phenology across the deciduous forests of the Eastern USA. *Agricultural
and Forest Meteorology*, 157, 96-105.
- Dragoni, D., Schmid, H.P., Wayson, C.A., Potter, H., Grimmond, C.S.B. and Randolph, J.C., 2011. Evidence of increased
735 net ecosystem productivity associated with a longer vegetated season in a deciduous forest in south-central Indiana, USA.
Global Change Biology, 17(2), 886-897.
- Dunn, A.L., Barford, C.C., Wofsy, S.C., Goulden, M.L. and Daube, B.C., 2007. A long-term record of carbon exchange in a
boreal black spruce forest: Means, responses to interannual variability, and decadal trends. *Global Change Biol.*, 13(3),
577-590.
- 740 Dymond, C.C., Beukema, S., Nitschke, C.R., Coates, K.D. and Scheller, R.M., 2016. Carbon sequestration in managed
temperate coniferous forests under climate change. *Biogeosciences*, 13, 1933-1947.
- Elliott, K., McCracken, J.D. and Couturier, A., 1999. A Management Strategy for South Walsingham Sand Ridges/Big
Creek Floodplain Forest. *Ont. Min. Nat. Resources*. London, Ontario. 54.
- Elliott, K.J., Vose, J.M., Knoepp, J.D., Clinton, B.D. and Kloeppel, B.D., 2015. Functional role of the herbaceous layer in
eastern deciduous forest ecosystems. *Ecosystems*, 18, 221-236.
- 745 Froelich, N., Croft, H., Chen, J.M., Gonsamo, A. and Staebler, R.M., 2015. Trends of carbon fluxes and climate over a
mixed temperate–boreal transition forest in southern Ontario, Canada. *Agricultural and Forest Meteorology*, 211, 72-84.
- Gallinat, A.S., Primack, R.B. and Wagner, D.L., 2015. Autumn, the neglected season in climate change research. *Trends in
Ecology & Evolution*, 30(3), 169-176.
- 750 Gaumont-Guay, D., Black, T.A., McCaughey, H., Barr, A.G., Krishnan, P., Jassal, R.S. and Nescic, Z., 2009. Soil CO₂ efflux
in contrasting boreal deciduous and coniferous stands and its contribution to the ecosystem carbon balance. *Glob. Change
Biol.*, 15, 1302-1319.
- Givnish, T.J., 2002. Adaptive significance of evergreen vs. deciduous leaves: solving the triple paradox. *Silva Fennica*,
36(3), 703-743.



- 755 Gonsamo, A., Chen, J.M. and D'Odorico, P., 2013. Deriving land surface phenology indicators from CO₂ eddy covariance measurements. *Ecological Indicators*, 29, 203-207.
- Gonsamo, A., Croft, H., Chen, J.M., Wu, C., Froelich, N. and Staebler, R.M., 2015. Radiation contributed more than temperature to increased decadal autumn and annual carbon uptake of two eastern North America mature forests. *Agric. For. Meteorol.*, 201, 8-16.
- 760 Gough, C.M., Hardiman, B.S., Nave, L.E., Bohrer, G., Maurer, K.D., Vogel, C.S., Nadelhoffer, K.J. and Curtis, P.S., 2013. Sustained carbon uptake and storage following moderate disturbance in a Great Lakes forest. *Ecological Applications*, 23(5), 1202-1215.
- Granier, A., Reichstein, M., Bréda, N., Janssens, I.A., Falge, E., Ciais, P., Grünwald, T., Aubinet, M., Berbigier, P., Bernhofer, C. and Buchmann, N., 2007. Evidence for soil water control on carbon and water dynamics in European forests during the extremely dry year: 2003. *Agricultural and Forest Meteorology*, 143(1-2), 123-145.
- 765 Grant, R.F., Barr, A.G., Black, T.A., Margolis, H.A., Dunn, A.L., Metsaranta, J., Wang, S., McCaughey, J.H. and Bourque, C.A., 2009. Interannual variation in net ecosystem productivity of Canadian forests as affected by regional weather patterns—A Fluxnet-Canada synthesis. *Agricultural and Forest Meteorology*, 149(11), 2022-2039.
- Griffis, T.J., Black, T.A., Morgenstern, K., Barr, A.G., Nescic, Z., Drewitt, G.B., Gaumont-Guay, D. and McCaughey, J.H., 2003. Ecophysiological controls on the carbon balances of three southern boreal forests. *Agricultural and Forest Meteorology*, 117(1-2), 53-71.
- 770 Gu, L., Post, W.M., Baldocchi, D.D., Black, T.A., Suyker, A.E., Verma, S.B., Vesala, T. and Wofsy, S.C., 2009. Characterizing the seasonal dynamics of plant community photosynthesis across a range of vegetation types. In *Phenology of Ecosystem Processes (35-58)*. Springer, New York, NY.
- 775 Herbst, M., Mund, M., Tamrakar, R. and Knohl, A., 2015. Differences in carbon uptake and water use between a managed and an unmanaged beech forest in central Germany. *Forest Ecology and Management*, 355, 101-108.
- Houghton, R.A., 2007. Balancing the global carbon budget. *Annual Review of Earth and Planetary Sciences*, 35, 313-347.
- Huntington, T.G., 2006. Evidence for intensification of the global water cycle: review and synthesis. *Journal of Hydrology*, 319(1-4), 83-95.
- 780 Ibáñez, I., Primack, R.B., Miller-Rushing, A.J., Ellwood, E., Higuchi, H., Lee, S.D., Kobori, H. and Silander, J.A., 2010. Forecasting phenology under global warming. *Philos. Trans. R. Soc. London, Ser. B*, 365(1555), 3247-3260.
- Jenkins, J.P., Richardson, A.D., Braswell, B.H., Ollinger, S.V., Hollinger, D.Y. and Smith, M.L., 2007. Refining light-use efficiency calculations for a deciduous forest canopy using simultaneous tower-based carbon flux and radiometric measurements. *Agricultural and Forest Meteorology*, 143(1-2), 64-79.
- 785 Jeong, S.J., Ho, C.H., Gim, H.J. and Brown, M.E., 2011. Phenology shifts at start vs. end of growing season in temperate vegetation over the Northern Hemisphere for the period 1982–2008. *Global Change Biology*, 17(7), 2385-2399.
- Keenan, T.F., Hollinger, D.Y., Bohrer, G., Dragoni, D., Munger, J.W., Schmid, H.P. and Richardson, A.D., 2013. Increase in forest water-use efficiency as atmospheric carbon dioxide concentrations rise. *Nature*, 499(7458), 324.
- 790 Kelliher, F.M., Leuning, R. and Schulze, E.D., 1993. Evaporation and canopy characteristics of coniferous forests and grasslands. *Oecologia*, 95(2), 153-163.
- Kljun, N., Calanca, P., Rotach, M.W., Schmid, H.P., 2004. A simple parametrization for flux footprint predictions. *Boundary-Layer Meteorology*, 112, 503–523.
- Kramer, K., Degen, B., Buschbom, J., Hickler, T., Thuiller, W., Sykes, M.T. and de Winter, W., 2010. Modelling explorationa of the future of European beech (*Fagussylvatica* L.) under climate change—Range, abundance, genetic diversity and adaptive response. *Forest Ecol. Manag.*, 259(11), 2213-2222.
- 795 Kula, M.V., 2014. Biometric-based carbon estimates and environmental controls within an age-sequence of temperate forests (Doctoral Dissertation), McMaster University.
- Lee, N.Y., Koo, J.W., Noh, N.J., Kim, J. and Son, Y., 2010. Seasonal variations in soil CO₂ efflux in evergreen coniferous and broad-leaved deciduous forests in a cool-temperate forest, central Korea. *Ecological Research*, 25, 609– 617.
- 800 Litton, C.M. and Giardina, C.P., 2008. Below-ground carbon flux and partitioning: Global patterns and response to temperature. *Functional Ecology*, 22(6), 941-954.



- Liu, K.B., 1990. Holocene paleoecology of the boreal forest and Great Lakes-St. Lawrence forest in northern Ontario. *Ecological Monographs*, 60(2), 179-212.
- 805 Liu, P., Black, T.A., Jassal, R.S., Zha, T., Nesic, Z., Barr, A.G., Helgason, W.D., Jia, X., Tian, Y., Stephens, J.J. and Ma, J., 2019. Divergent long-term trends and interannual variation in ecosystem resource use efficiencies of a southern boreal old black spruce forest 1999– 2017. *Global Change Biology*, 25: 3056-3069.
- Liu, Q., Fu, Y.H., Zhu, Z., Liu, Y., Liu, Z., Huang, M., Janssens, I.A. and Piao, S., 2016. Delayed autumn phenology in the Northern Hemisphere is related to change in both climate and spring phenology. *Global Change Biology*, 22(11), 3702-3711.
- 810 M. Altaf Arain (2003-) AmeriFlux CA-TP4 Ontario - Turkey Point 1939 Plantation White Pine, 10.17190/AMF/1246012.
M. Altaf Arain (2012-) AmeriFlux CA-TPD Ontario - Turkey Point Mature Deciduous, 10.17190/AMF/1246152.
- MacKay, S.L., Arain, M.A., Khomik, M., Brodeur, J.J., Schumacher, J., Hartmann, H. and Peichl, M., 2012. The impact of induced drought on transpiration and growth in a temperate pine plantation forest. *Hydrological Processes*, 26(12), 1779-1791.
- 815 Matheny, A.M., Fiorella, R.P., Bohrer, G., Poulsen, C.J., Morin, T.H., Wunderlich, A., Vogel, C.S. and Curtis, P.S., 2017. Contrasting strategies of hydraulic control in two codominant temperate tree species. *Ecohydrology*, 10(3), 1815.
- McLaren, J.D., Arain, M.A., Khomik, M., Peichl, M. and Brodeur, J., 2008. Water flux components and soil water-atmospheric controls in a temperate pine forest growing in a well-drained sandy soil. *Journal of Geophysical Research: Biogeosciences*, 113(G4).
- 820 Meinzer, F.C., Woodruff, D.R., Eissenstat, D.M., Lin, H.S., Adams, T.S. and McCulloh, K.A., 2013. Above-and belowground controls on water use by trees of different wood types in an eastern US deciduous forest. *Tree Physiology*, 33(4), 345-356.
- Morin, X., Fahse, L., Scherer-Lorenzen, M. and Bugmann, H., 2011. Tree species richness promotes productivity in temperate forests through strong complementarity between species. *Ecology Letters*, 14(12), 1211-1219.
- 825 Nemani, R.R., Keeling, C.D., Hashimoto, H., Jolly, W.M., Piper, S.C., Tucker, C.J., Myneni, R.B. and Running, S.W., 2003. Climate-driven increases in global terrestrial net primary production from 1982 to 1999. *Science*, 300(5625), 1560-1563.
- Noormets, A., Epron, D., Domec, J.C., McNulty, S.G., Fox, T., Sun, G. and King, J.S., 2015. Effects of forest management on productivity and carbon sequestration: A review and hypothesis. *Forest Ecology and Management*, 355, 124-140.
- 830 Novick, K.A., Oishi, A.C., Ward, E.J., Siqueira, M.B., Juang, J.Y. and Stoy, P.C., 2015. On the difference in the net ecosystem exchange of CO₂ between deciduous and evergreen forests in the southeastern United States. *Global Change Biology*, 21(2), 827-842.
- Oishi, A.C., Miniati, C.F., Novick, K.A., Brantley, S.T., Vose, J.M. and Walker, J.T., 2018. Warmer temperatures reduce net carbon uptake, but do not affect water use, in a mature southern Appalachian forest. *Agricultural and Forest Meteorology*, 252, 269-282.
- 835 Oren, R. and Pataki, D.E., 2001. Transpiration in response to variation in microclimate and soil moisture in southeastern deciduous forests. *Oecologia*, 127(4), 549-559.
- Palmroth, S., Maier, C.A., McCarthy, H.R., Oishi, A.C., Kim, H.S., Johnsen, K.H., et al., 2005. Contrasting responses to drought of forest floor CO₂ efflux in a loblolly pine plantation and a nearby oak-hickory forest. *Global Change Biology*, 11(3), 421-434.
- 840 Papale, D., Reichstein, M., Aubinet, M., Canfora, E., Bernhofer, C., Kutsch, W., Longdoz, B., Rambal, S., Valentini, R., Vesala, T., Yakir, D., 2006. Towards a standardized processing of Net Ecosystem Exchange measured with eddy covariance technique: algorithms and uncertainty estimation. *Biogeosciences*, 3, 571–583.
- Peichl, M. and Arain, M.A., 2007. Allometry and partitioning of above-and belowground tree biomass in an age-sequence of white pine forests. *For. Ecol. Manag.*, 253(1-3), 68-80.
- 845 Peichl, M., Arain, M.A. and Brodeur, J.J., 2010a. Age effects on carbon fluxes in temperate pine forests. *Agricultural and Forest Meteorology*, 150(7-8), 1090-1101.
- Piao, S., Ciais, P., Friedlingstein, P., Peylin, P., Reichstein, M., Luysaert, S., Margolis, H., Fang, J., Barr, A., Chen, A. and Grelle, A., 2008. Net carbon dioxide losses of northern ecosystems in response to autumn warming. *Nature*, 451(7174), 49.
- 850 Pretzsch, H., 2014. Canopy space filling and tree crown morphology in mixed-species stands compared with monocultures. *Forest Ecology and Management*, 327, 251-264.



- Polgar, C.A. and Primack, R.B., 2011. Leaf-out phenology of temperate woody plants: from trees to ecosystems. *New Phytologist*, 191(4), 926-941.
- 855 Rambal, S., Ourcival, J.M., Joffre, R., Mouillot, F., Nouvellon, Y., Reichstein, M. and Rocheteau, A., 2003. Drought controls over conductance and assimilation of a Mediterranean evergreen ecosystem: scaling from leaf to canopy. *Global Change Biology*, 9(12), 1813-1824.
- Reich, P.B., Walters, M.B., Kloeppel, B.D. and Ellsworth, D.S., 1995. Different photosynthesis-nitrogen relations in deciduous hardwood and evergreen coniferous tree species. *Oecologia*, 104(1), 24-30.
- 860 Reichstein, M., Falge, E., Baldocchi, D., Papale, D., Aubinet, M., et al., 2005. On the separation of net ecosystem exchange into assimilation and ecosystem respiration: review and improved algorithm. *Glob. Chang. Biol.*, 11, 1424-1439.
- Richart, M. and Hewitt, N., 2008. Forest remnants in the Long Point region, Southern Ontario: Tree species diversity and size structure. *Landscape and Urban Planning*, 86(1), 25-37.
- Sanz-Pérez, V., Castro-Díez, P. and Valladares, F., 2009. Differential and interactive effects of temperature and photoperiod on budburst and carbon reserves in two co-occurring Mediterranean oaks. *Plant Biology*, 11(2), 142-151.
- 865 Schwartz, M.D., Ahas, R. and Aasa, A., 2006. Onset of spring starting earlier across the Northern Hemisphere. *Global Change Biology*, 12(2), 343-351.
- Settele, J., R. Scholes, R. Betts, S. Bunn, P. Leadley, D. Nepstad, J.T. Overpeck, and M.A. Taboada, 2014: Terrestrial and inland water systems. *Climate Change 2014: Impacts, Adaptation, and Vulnerability. Part A: Global and Sectoral Aspects. Contribution of Working Group II to the Fifth Assessment Report of the Intergovernmental Panel on Climate Change* [Field, C.B., V.R. Barros, D.J. Dokken, K.J. Mach, M.D. Mastrandrea, T.E. Bilir, et al (eds.)]. Cambridge University Press, New York, NY, USA, 271-359.
- 870 Skubel, R., Arain, M.A., Peichl, M., Brodeur, J.J., Khomik, M., Thorne, R., Trant, J. and Kula, M., 2015. Age effects on the water-use efficiency and water-use dynamics of temperate pine plantation forests. *Hydrological Processes*, 29(18), 4100-4113.
- 875 Skubel, R.A., Khomik, M., Brodeur, J.J., Thorne, R. and Arain, M.A., 2017. Short-term selective thinning effects on hydraulic functionality of a temperate pine forest in eastern Canada. *Ecohydrology*, 10(1), e1780.
- Song, C. and Woodcock, C.E., 2003. A regional forest ecosystem carbon budget model: impacts of forest age structure and landuse history. *Ecological Modelling*, 164(1), 33-47.
- 880 Stokes, V.J., Morecroft, M.D. and Morison, J.I., 2006. Boundary layer conductance for contrasting leaf shapes in a deciduous broadleaved forest canopy. *Agricultural and Forest Meteorology*, 139(1-2), 40-54.
- Stoy, P.C., Katul, G.G., Siqueira, M.B., Juang, J.Y., Novick, K.A., McCarthy, H.R., Oishi, A.C., Uebelherr, J.M., Kim, H.S. and Oren, R.A.M., 2006. Separating the effects of climate and vegetation on evapotranspiration along a successional chronosequence in the southeastern US. *Global Change Biology*, 12(11), 2115-2135.
- 885 Sun, G., Caldwell, P., Noormets, A., McNulty, S.G., Cohen, E., Moore Myers, J., Domec, J.C., Treasure, E., Mu, Q., Xiao, J. and John, R., 2011. Upscaling key ecosystem functions across the conterminous United States by a water-centric ecosystem model. *Journal of Geophysical Research: Biogeosciences*, 116(G3).
- Tang, Y., Wen, X., Sun, X., Zhang, X. and Wang, H., 2014. The limiting effect of deep soilwater on evapotranspiration of a subtropical coniferous plantation subjected to seasonal drought. *Advances in Atmospheric Sciences*, 31(2), 385-395.
- 890 Taylor, G., Tallis, M.J., Giardina, C.P., Percy, K.E., Miglietta, F., Gupta, P.S., Gioli, B., Calfapietra, C., Gielen, B., Kubiske, M.E. and Scarascia-Mugnozza, G.E., 2008. Future atmospheric CO₂ leads to delayed autumnal senescence. *Glob. Change Biol*, 14, 264-275.
- Teskey, R., Wertin, T., Bauweraerts, I., Ameye, M., McGuire, M.A. and Steppe, K., 2015. Responses of tree species to heat waves and extreme heat events. *Plant, Cell & Environment*, 38(9), 1699-1712.
- 895 Vargas, R., Sonnentag, O., Abramowitz, G., Carrara, A., Chen, J.M., Ciais, P., Correia, A., Keenan, T.F., Kobayashi, H., Ourcival, J.M. and Papale, D., 2013. Drought influences the accuracy of simulated ecosystem fluxes: a model-data meta-analysis for Mediterranean oak woodlands. *Ecosystems*, 16(5), 749-764.
- Vitasse, Y., François, C., Delpierre, N., Dufrene, E., Kremer, A., Chuine, I. and Delzon, S., 2011. Assessing the effects of climate change on the phenology of European temperate trees. *Agricultural and Forest Meteorology*, 151(7), 969-980.
- 900 Wagle, P., Xiao, X., Kolb, T.E., Law, B.E., Wharton, S., Monson, R.K., Chen, J., Blanken, P.D., Novick, K.A., Dore, S. and Noormets, A., 2016. Differential responses of carbon and water vapor fluxes to climate among evergreen needleleaf forests in the USA. *Ecological Processes*, 5(1), 8.



- 905 Wang, J., Xiao, X., Wagle, P., Ma, S., Baldocchi, D., Carrara, A., Zhang, Y., Dong, J. and Qin, Y., 2016. Canopy and climate controls of gross primary production of Mediterranean-type deciduous and evergreen oak savannas. *Agric. For. Meteorol.*, 226, 132-147.
- Warren, J.M., Norby, R.J. and Wullschleger, S.D., 2011. Elevated CO₂ enhances leaf senescence during extreme drought in a temperate forest. *Tree Physiology*, 31(2), 117-130.
- Way, D.A. and Oren, R., 2010. Differential responses to changes in growth temperature between trees from different functional groups and biomes: a review and synthesis of data. *Tree Physiology*, 30(6), 669-688.
- 910 Weed, A.S., Ayres, M.P. and Hicke, J.A., 2013. Consequences of climate change for biotic disturbances in North American forests. *Ecological Monographs*, 83(4), 441-470.
- White, M.A. and Nemani, R.R., 2003. Canopy duration has little influence on annual carbon storage in the deciduous broad leaf forest. *Global Change Biol.*, 9(7), 967-972.
- 915 Wiken, E.D., Nava, F.J. and Griffith, G., 2011. North American Terrestrial Ecoregions—Level III. Commission for Environmental Cooperation, Montreal, Canada, 149.
- Wofsy, S.C., Goulden, M.L., Munger, J.W., Fan, S.M., Bakwin, P.S., Daube, B.C., Bassow, S.L. and Bazzaz, F.A., 1993. Net exchange of CO₂ in a mid-latitude forest. *Science*, 260(5112), 1314-1317.
- Wolf, S., Eugster, W., Ammann, C., Häni, M., Zielis, S., Hiller, R., et al., 2013. Contrasting response of grassland versus forest carbon and water fluxes to spring drought in Switzerland. *Environmental Research Letters*, 8(3), 035007.
- 920 Wu, J., Jing, Y., Guan, D., Yang, H., Niu, L., Wang, A., et al., 2013. Controls of evapotranspiration during the short dry season in a temperate mixed forest in Northeast China. *Ecohydrology*, 6(5), 775-782.
- Xie, J., Chen, J., Sun, G., Chu, H., Noormets, A., Ouyang, Z., John, R., Wan, S. and Guan, W., 2014. Long-term variability and environmental control of the carbon cycle in an oak-dominated temperate forest. *Forest Ecology and Management*, 313, 319-328.
- 925 Xie, J., Chen, J., Sun, G., Zha, T., Yang, B., Chu, H., Liu, J., Wan, S., Zhou, C., Ma, H. and Bourque, C.P.A., 2016. Ten-year variability in ecosystem water use efficiency in an oak-dominated temperate forest under a warming climate. *Agricultural and Forest Meteorology*, 218, 209-217.
- Yuan, W., Luo, Y., Richardson, A.D., Oren, R.A.M., Luysaert, S., Janssens, I.A., Ceulemans, R., Zhou, X., Grünwald, T., Aubinet, M. and Berhofer, C., 2009. Latitudinal patterns of magnitude and interannual variability in net ecosystem exchange regulated by biological and environmental variables. *Global Change Biology*, 15(12), 2905-2920.
- 930 Zha, T., Barr, A.G., Black, T.A., McCaughey, J.H., Bhatti, J., Hawthorne, I., Krishnan, P., Kidston, J., Saigusa, N., Shashkov, A. and Nesic, Z., 2009. Carbon sequestration in boreal jack pine stands following harvesting. *Global Change Biology*, 15(6), 1475-1487.

935

940

945



Table 1. Site characteristics of the deciduous (TPD) and coniferous (TP39) forest stands. The TP39 values in brackets indicate pre-thinning (2003 – 2011) values, prior to the period of focus.

	Turkey Point 1939 (TP39)	Turkey Point Deciduous (TPD)
	42.71°N, 80.357°W	42.635°N, 80.558°W
Stand	Afforested on oak savanna,	Naturally regenerated on
Previous Land Use	cleared for afforestation	abandoned agricultural land
Age (in 2017)	78 years	70 – 110 years
Elevation (m)	184	265
DBH (cm)	39.0 (37.2)	23.1
Density (trees ha ⁻¹)	321 (413)	504
Tree Height (m)	23.4 (22.9)	25.7
LAI (m ² m ⁻²)	5.3 (8.5)	8.0
Dominant Species	<i>Pinus Stobus L.</i>	<i>Quercus Alba</i>
Secondary & Understory	<i>Abies Balsamea, Q. Velutina, A. Rubrum, Prunus Serotina</i>	<i>Acer Saccharum, A. Rubrum, Fagus Grandifolia, Q. Velutina, Q. Rubra, Fraxinus Americana</i>
Ground	<i>M. Canadense, Rubus Spp., Rhus Radicans, Ferns, Mosses</i>	<i>Maianthemum Canadense, Aplectrum Hyemale, Equisetum</i>
Soil		
Drainage	Well-drained	Rapid to well-drained
Classification	Brunisolic grey brown luvisol	Brunisolic grey brown luvisol
Texture	Very fine sandy-loam	Predominantly sandy
Bulk Density (kg m ⁻³)	1.35 g m ⁻³	1.15 g m ⁻³

950

955



960

Table 2. The top section of the table contains the annual calculated phenological dates (reported as day of year) for both the conifer (TP39, **bolded C**) and deciduous (TPD, *italicized D*) forests from year 2012 to year 2017. Phenological dates were calculated following Gonsamo et al. (2013) from eddy covariance measured GEP_{Max} data. The six-year mean values and standard deviations are included in the final column. The resulting phenological periods (seasons) and their duration in days are also shown, in the lower section of the table.

Phenology Transition Dates		2012	2013	2014	2015	2016	2017	Mean
Start of Season (SOS, bud-break)	C <i>D</i>	70 120	96 116	96 127	91 118	74 126	79 125	84 ± 12 122 ± 5
Mid of Greenup (MOG, fastest green-up)	C <i>D</i>	119 136	137 141	132 148	122 136	127 144	130 147	128 ± 7 142 ± 5
End of Greenup (EOG, end of leaf-out)	C <i>D</i>	147 145	160 155	153 160	140 146	158 154	159 159	153 ± 8 153 ± 6
Peak of Season (Midpoint between EOG & SOB)	C <i>D</i>	214 198	205 199	202 205	193 193	212 203	201 207	204 ± 8 201 ± 5
Start of Browndown (SOB, start of senescence)	C <i>D</i>	271 257	258 249	258 255	257 249	270 262	248 261	260 ± 9 255 ± 6
Mid of Browndown (MOB, fastest senescence)	C <i>D</i>	287 275	292 273	287 274	289 271	305 286	287 282	291 ± 7 277 ± 6
End of Season (EOS)	C <i>D</i>	314 306	351 314	338 307	345 309	366 328	354 318	345 ± 17 314 ± 8
Phenologically-Defined Seasons		2012	2013	2014	2015	2016	2017	Mean
Spring (EOG – SOS)	C <i>D</i>	78 25	64 39	58 34	48 28	84 28	80 34	69 ± 14 31 ± 5
Summer (SOB – EOG) (LOCC, Length of Canopy Closure)	C <i>D</i>	124 112	97 94	105 95	117 103	112 107	89 102	107 ± 13 102 ± 7
Autumn (EOS – SOB)	C <i>D</i>	43 49	94 65	80 52	89 61	96 67	106 57	85 ± 22 58 ± 7
Length of Growing Season (LOS)	C <i>D</i>	245 186	255 198	242 180	254 191	292 202	275 193	260 ± 19 192 ± 8

965

970



Table 3. Seasonal and annual sums of eddy covariance (EC) measured carbon (GEP, RE, and NEP, $\text{g C m}^{-2} \text{yr}^{-1}$) and water fluxes (ET, mm yr^{-1}) from 2012 to 2017 for both the conifer (TP39, **bolded C**) and deciduous (TPD, *italicized D*) forests. The phenologically-defined seasonal dates were calculated using the timing of transitions in phenological dates, outlined in Table 2. The six-year mean and standard deviations are also included for each row.

975

Season		2012	2013	2014	2015	2016	2017	Mean
GEP Sum	Jan 1 to SOS	--	--	--	--	--	--	--
	Spring (SOS to EOG)	C 308	306	279	213	359	418	314 ± 70
		<i>D 104</i>	<i>197</i>	<i>165</i>	<i>117</i>	<i>129</i>	<i>174</i>	<i>148 ± 36</i>
	Summer (EOG to SOB)	C 990	942	1070	1160	1014	930	1018 ± 86
		<i>D 942</i>	<i>949</i>	<i>1023</i>	<i>1006</i>	<i>1084</i>	<i>1070</i>	<i>1012 ± 59</i>
	Autumn (SOB to EOS)	C 132	264	265	340	249	377	271 ± 85
		<i>D 147</i>	<i>239</i>	<i>200</i>	<i>240</i>	<i>219</i>	<i>213</i>	<i>210 ± 34</i>
EOS to Dec 31	--	--	--	--	--	--	--	
Annual	C	1452	1501	1601	1701	1617	1709	1597 ± 104
	<i>D</i>	<i>1198</i>	<i>1369</i>	<i>1382</i>	<i>1347</i>	<i>1420</i>	<i>1447</i>	<i>1360 ± 87</i>
RE Sum	Jan 1 to SOS	C 66	83	78	79	82	81	78 ± 6
		<i>D 167</i>	<i>107</i>	<i>129</i>	<i>109</i>	<i>163</i>	<i>170</i>	<i>141 ± 30</i>
	Spring (SOS to EOG)	C 205	205	169	122	233	276	202 ± 53
		<i>D 78</i>	<i>151</i>	<i>133</i>	<i>109</i>	<i>109</i>	<i>144</i>	<i>121 ± 27</i>
	Summer (EOG to SOB)	C 908	718	809	790	888	735	808 ± 78
		<i>D 500</i>	<i>672</i>	<i>581</i>	<i>714</i>	<i>684</i>	<i>700</i>	<i>642 ± 84</i>
	Autumn (SOB to EOS)	C 142	272	269	310	302	434	288 ± 94
	<i>D 138</i>	<i>269</i>	<i>196</i>	<i>259</i>	<i>266</i>	<i>252</i>	<i>230 ± 52</i>	
EOS to Dec 31	C 77	14	33	39	--	13	35 ± 26	
	<i>D 82</i>	<i>64</i>	<i>84</i>	<i>110</i>	<i>55</i>	<i>65</i>	<i>77 ± 20</i>	
Annual	C	1386	1282	1345	1328	1492	1525	1393 ± 96
	<i>D</i>	<i>954</i>	<i>1250</i>	<i>1110</i>	<i>1283</i>	<i>1260</i>	<i>1317</i>	<i>1196 ± 138</i>
NEP Sum	Jan 1 to SOS	C -58	-74	-68	-73	-66	-66	-67 ± 6
		<i>D -117</i>	<i>-79</i>	<i>-88</i>	<i>-82</i>	<i>-129</i>	<i>-130</i>	<i>-104 ± 24</i>
	Spring (SOS to EOG)	C 103	101	110	92	128	144	113 ± 19
		<i>D 25</i>	<i>45</i>	<i>30</i>	<i>4</i>	<i>18</i>	<i>29</i>	<i>25 ± 14</i>
	Summer (EOG to SOB)	C 80	223	262	374	127	196	210 ± 104
		<i>D 442</i>	<i>276</i>	<i>441</i>	<i>288</i>	<i>398</i>	<i>371</i>	<i>369 ± 73</i>
	Autumn (SOB to EOS)	C -12	-5	-6	33	-48	-51	-15 ± 31
	<i>D 16</i>	<i>-26</i>	<i>4</i>	<i>-18</i>	<i>-46</i>	<i>-37</i>	<i>-18 ± 24</i>	
EOS to Dec 31	C -35	-12	-30	-24	--	-12	-23 ± 10	
	<i>D -68</i>	<i>-56</i>	<i>-79</i>	<i>-103</i>	<i>-51</i>	<i>-58</i>	<i>-69 ± 19</i>	
Annual	C	76	228	263	395	139	208	218 ± 109
	<i>D</i>	<i>292</i>	<i>156</i>	<i>305</i>	<i>90</i>	<i>185</i>	<i>169</i>	<i>200 ± 83</i>
ET Sum	Jan 1 to SOS	C 22	23	11	19	13	15	17 ± 5
		<i>D 56</i>	<i>28</i>	<i>33</i>	<i>24</i>	<i>39</i>	<i>44</i>	<i>37 ± 12</i>
	Spring (SOS to EOG)	C 105	97	67	65	85	106	87 ± 18
		<i>D 36</i>	<i>55</i>	<i>45</i>	<i>31</i>	<i>39</i>	<i>48</i>	<i>42 ± 9</i>
	Summer (EOG to SOB)	C 315	277	260	286	249	210	266 ± 36
		<i>D 283</i>	<i>231</i>	<i>213</i>	<i>219</i>	<i>266</i>	<i>237</i>	<i>242 ± 27</i>
	Autumn (SOB to EOS)	C 43	73	82	67	64	97	71 ± 18
	<i>D 45</i>	<i>63</i>	<i>50</i>	<i>66</i>	<i>69</i>	<i>64</i>	<i>60 ± 9</i>	
EOS to Dec 31	C 15	2	6	4	--	3	6 ± 5	
	<i>D 14</i>	<i>9</i>	<i>12</i>	<i>14</i>	<i>11</i>	<i>15</i>	<i>12 ± 2</i>	
Annual	C	495	468	421	436	408	424	442 ± 33
	<i>D</i>	<i>428</i>	<i>381</i>	<i>350</i>	<i>349</i>	<i>417</i>	<i>403</i>	<i>388 ± 34</i>



980

Table 4. Linear relationships between total annual water (ET, mm yr⁻¹) and carbon (RE and NEP, g C m⁻² yr⁻¹) flux measurements and both meteorological (i.e. VPD, Ta, $\theta_{0-30\text{cm}}$) and phenological (i.e. spring length, carbon uptake start) variables (annual or seasonal) from 2012 to 2017. In each section, the R² is for the relationship to the specified annual flux.

Conifer	2012	2013	2014	2015	2016	2017	R²
Annual RE (g C m ⁻² yr ⁻¹)	1386	1282	1345	1328	1492	1525	--
Summer $\theta_{0-30\text{cm}}$ (m ³ m ⁻³)	0.083	0.097	0.090	0.096	0.071	0.076	0.89
Annual NEP (g C m ⁻² yr ⁻¹)	76	228	263	395	139	208	--
Spring Length (Days)	78	64	58	48	84	80	0.75
Summer Ta (°C)	21.1	20.3	19.9	20.0	21.1	20.7	0.73
Summer NEP (g C m ⁻²)	80	223	262	374	127	196	0.99
Deciduous	2012	2013	2014	2015	2016	2017	R²
Annual ET (mm yr ⁻¹)	428	381	350	349	417	403	--
Annual Ta (°C)	11.8	9.2	8.0	9.2	10.6	10.0	0.84
Winter $\theta_{0-30\text{cm}}$ (m ³ m ⁻³)	0.131	0.118	0.116	0.101	0.133	0.127	0.83
Annual RE (g C m ⁻² yr ⁻¹)	954	1250	1110	1283	1260	1317	--
Spring Ta (°C)	16.6	15.1	16.1	15.1	15.6	14.0	0.77
Annual NEP (g C m ⁻² yr ⁻¹)	292	156	305	90	185	169	--
Summer RE (g C m ⁻²)	500	672	581	714	684	700	0.80

985

990

995



1000 **Table 5.** The model-predicted scaling factors of meteorological variables (i.e. Ta, VPD, PAR, $\theta_{0-30\text{cm}}$) during the phenological summer (end of greenup to start of senescence) for the conifer and deciduous forests from 2012 to 2017. These normalized values show the cumulative effect of the meteorological variable in reducing GEP and RE from their theoretical maximum values. Higher values represent more favorable summer conditions for GEP and RE.

Conifer	2012	2013	2014	2015	2016	2017
GEP: Ta	0.994	0.990	0.987	0.981	1.00	0.997
GEP: VPD	0.939	1.00	1.00	0.981	0.914	0.975
GEP: PAR	0.949	0.950	0.946	0.956	1.00	0.950
GEP: $\theta_{0-30\text{cm}}$	0.956	1.00	0.998	0.993	0.976	0.973
GEP: All	0.846	0.941	0.932	0.914	0.892	0.899
RE: $\theta_{0-30\text{cm}}$	0.958	1.00	0.996	0.991	0.968	0.965
Deciduous	2012	2013	2014	2015	2016	2017
GEP: Ta	1.00	0.971	0.974	0.967	0.989	0.974
GEP: VPD	0.871	1.00	0.998	0.998	0.946	0.989
GEP: PAR	0.978	0.938	0.955	0.953	1.00	0.956
GEP: $\theta_{0-30\text{cm}}$	1.00	1.00	1.00	1.00	1.00	1.00
GEP: All	0.852	0.911	0.929	0.920	0.936	0.920
RE: $\theta_{0-30\text{cm}}$	0.976	1.00	0.997	1.00	0.965	0.992

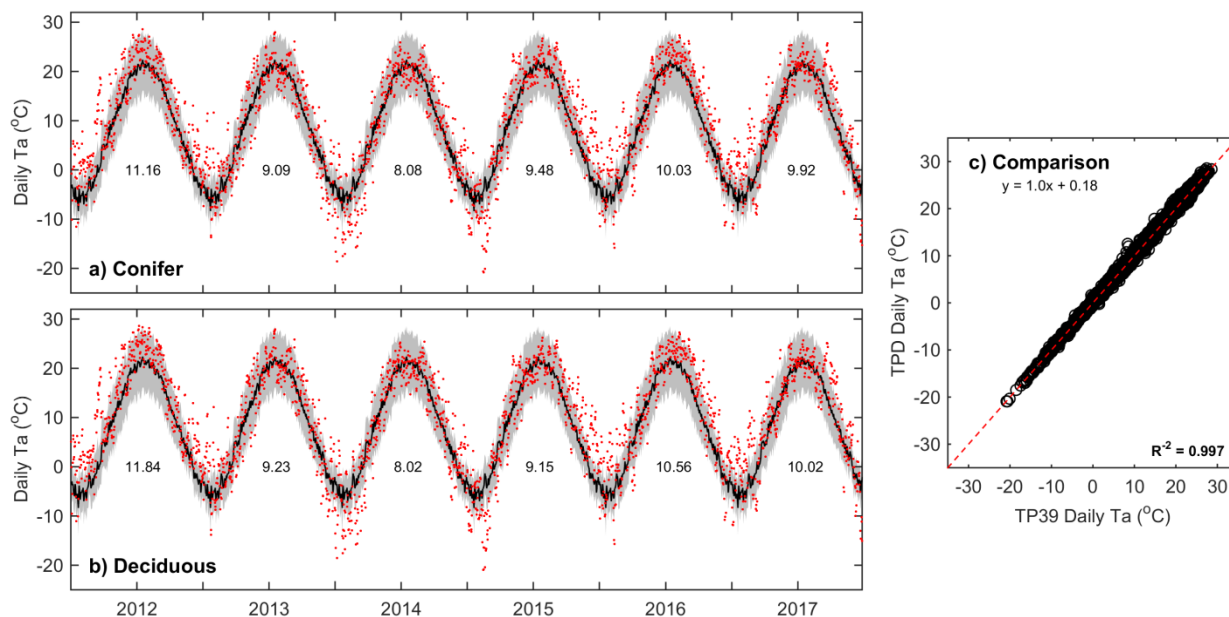
1005

1010

1015

1020

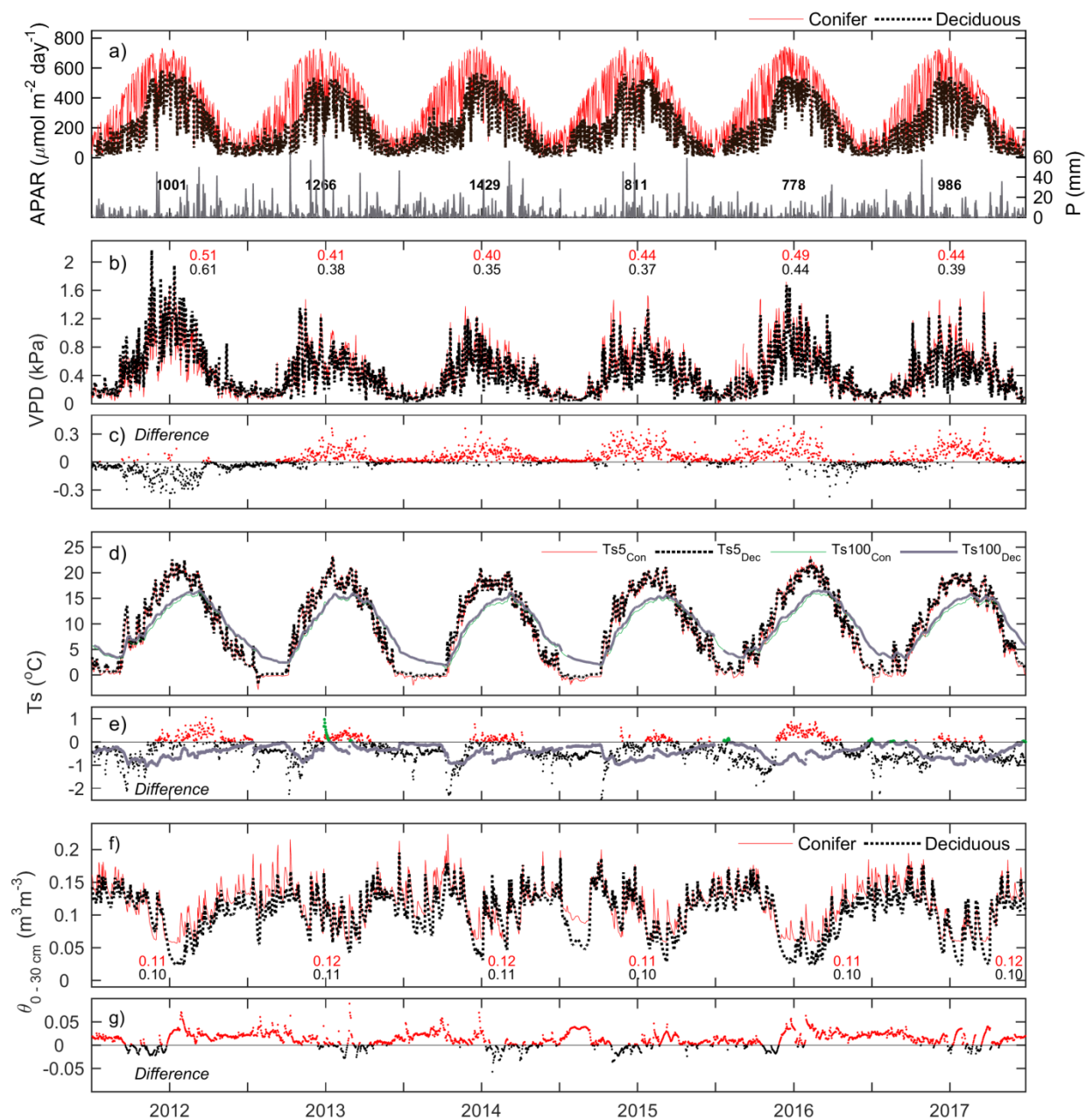
1025



1030 **Figure 1.** Daily above canopy air temperature (T_a , red dots) measured from 2012 to 2017 at the (a) conifer forest (TP39) and (b) deciduous forest (TPD), with the grey shading and black line corresponding to the 30-year Environment Canada (Delhi station) minimum and maximum range of daily T_a and mean daily T_a , respectively. Values shown represent the annual mean T_a for each year of measurements. Also included is the (c) comparison of daily T_a at TP39 and TPD.

1035

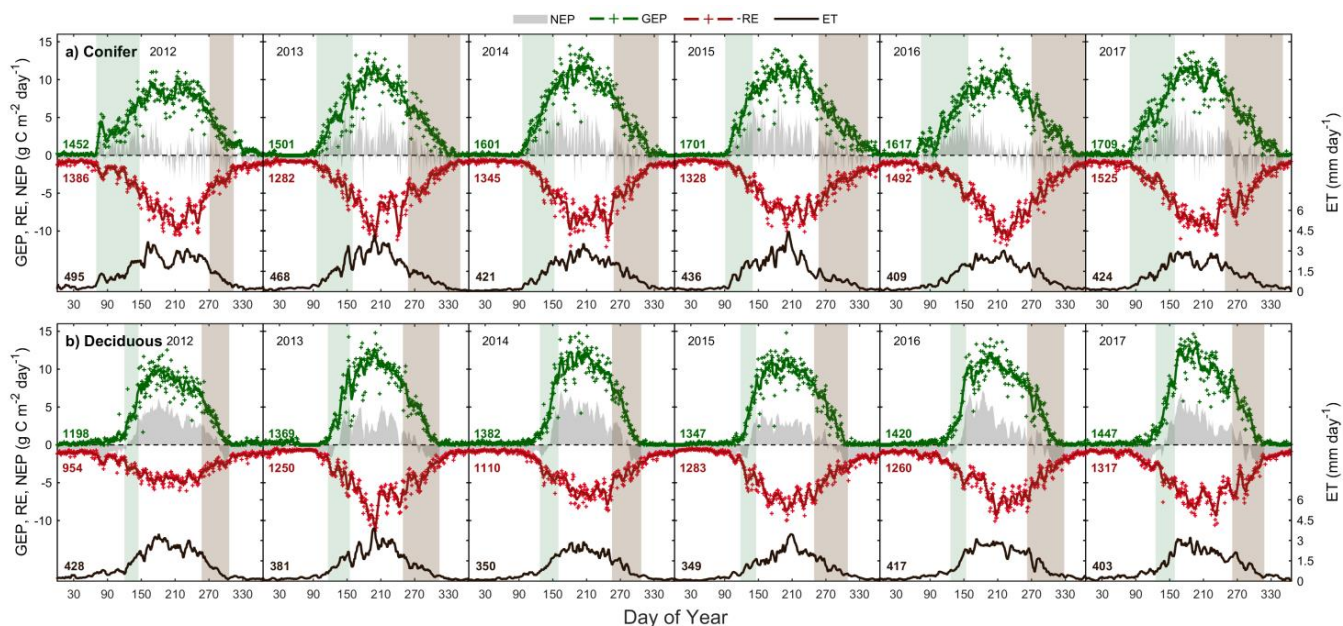
1040



1045

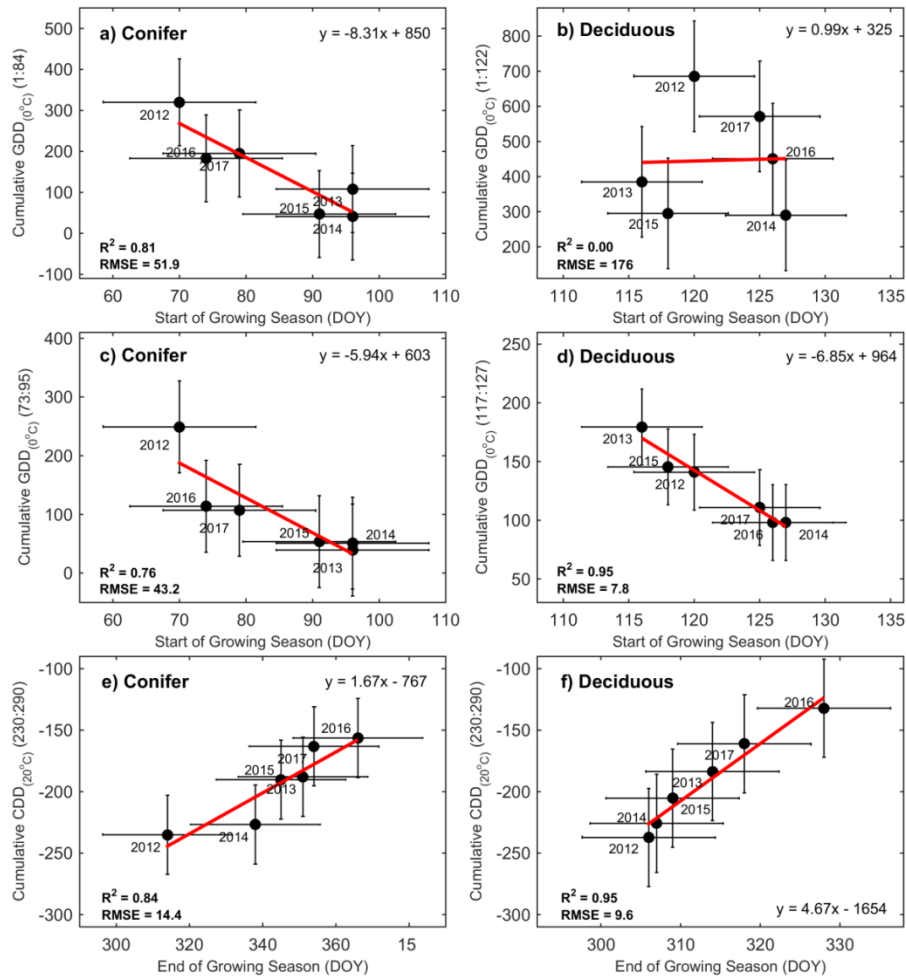
Figure 2. A daily time series of meteorological variables measured at the conifer (TP39, red line) and deciduous (TPD, black dashed line) forests from 2012 to 2017, including: (a, left) absorbed photosynthetically active radiation (APAR), (a, right) total precipitation (P), (b) vapor pressure deficit (VPD), (c) the difference in VPD between the two forests (conifer – deciduous), (d) soil temperatures (Ts) at 5 cm and 100 cm depths, (e) the difference in Ts at both depths, (f) soil volumetric water content from 0-30 cm depths ($\theta_{0-30\text{cm}}$), and (g) the difference in θ .

1050



1055 **Figure 3.** Time series from 2012 to 2017 of the daily total gross ecosystem productivity (GEP, green +), ecosystem
respiration (RE, red +), net ecosystem productivity (NEP, grey shading), and evapotranspiration (ET, black [right]) for the
(a) conifer forest (TP39), and the (b) deciduous forest (TPD). Solid lines of GEP, RE, NEP, and ET are derived from 5-day
moving averages of the measured data, while the colored values for each year correspond to annual GEP (green), RE (red),
and ET (black) for each site. The annual EC-derived phenological spring (green shading) and autumn (brown shading) are
included for each site, and can be found in Table 2.

1060



1065 **Figure 4.** Correlations between growing degree days (GDD), cooling degree days (CDD) and and phenological start of the
 growing season (SOS) and end of the growing season (EOS) from 2012 to 2017 at both the conifer and deciduous forests.
 Shown are: (a) cumulative GDD from January 1st to the mean SOS at TP39 and (b) TPD, (c) cumulative GDD from the mean
 SOS \pm standard deviation at TP39 and (d) TPD, and (e) the cumulative CDD from day of year 230:290 at TP39 and (f) TPD.
 Error bars represent the standard deviation of the data, with R^2 , RMSE, and linear fit equations included for each correlation.

1070

1075

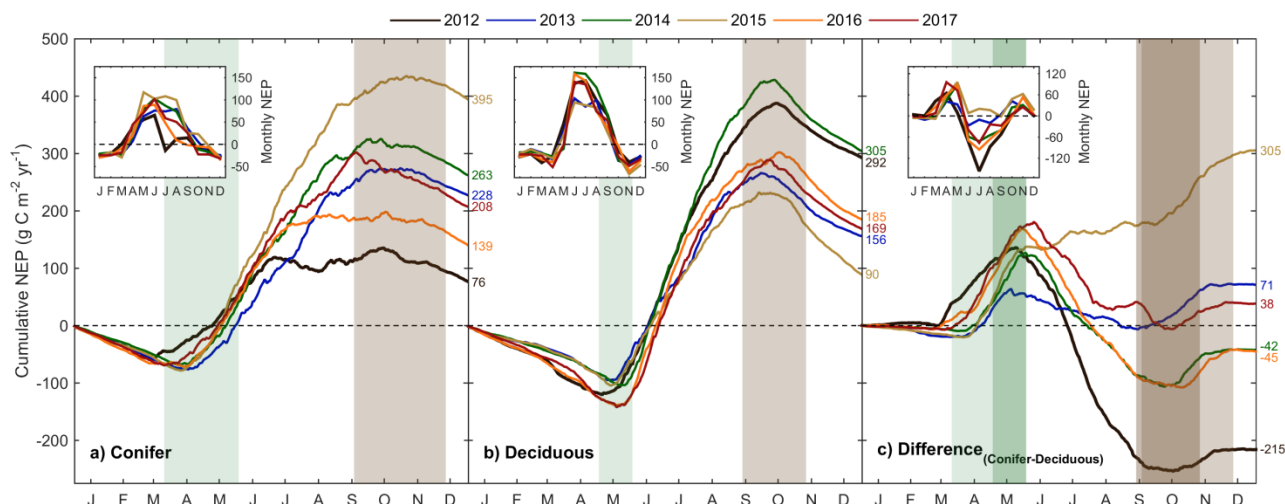


Figure 5. Cumulative daily sums of net ecosystem productivity (NEP) at the (a) conifer forest (TP39), the (b) deciduous forest (TPD), and (c) the cumulative difference (conifer – deciduous), with appropriate monthly NEP sums in each figure inset, from 2012 to 2017. Green shading in each panel corresponds to the site-specific 6-year mean phenological spring duration, while brown shading corresponds to the 6-year mean phenological autumn duration (Table 2). Dark shading in panel (c) represents the deciduous forest seasons overlaid on the conifer seasons. Cumulative annual values are shown for each site and year, with colors found in the key.

1085

1090

1095

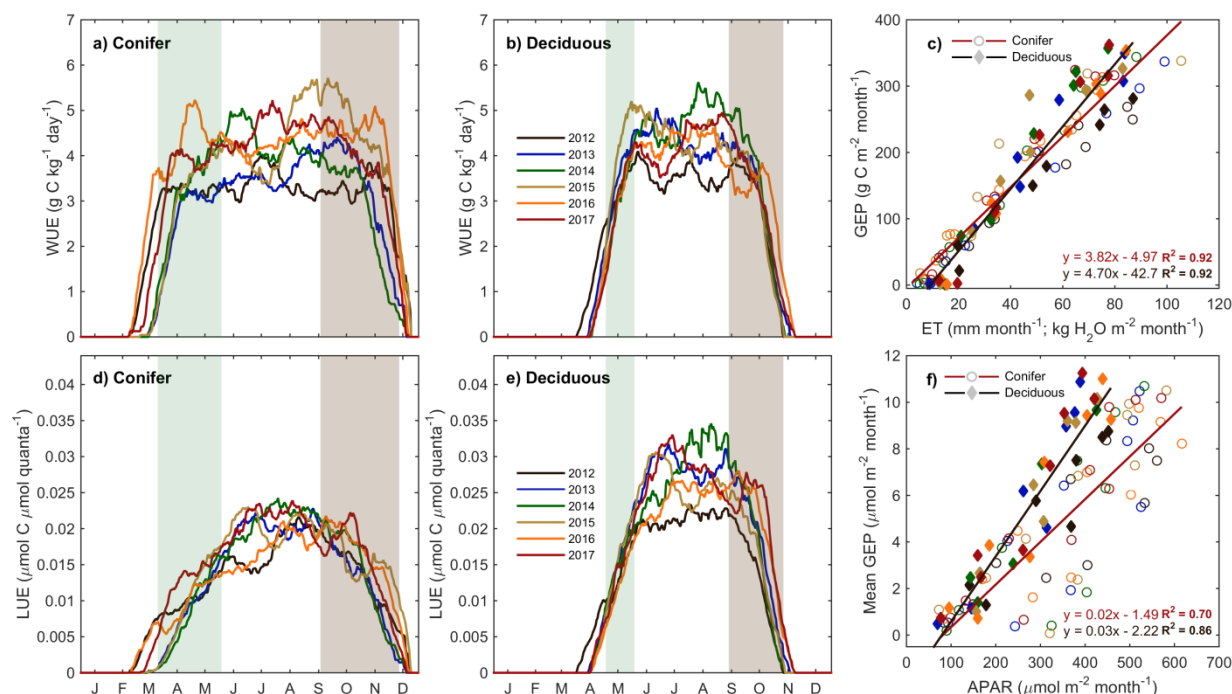
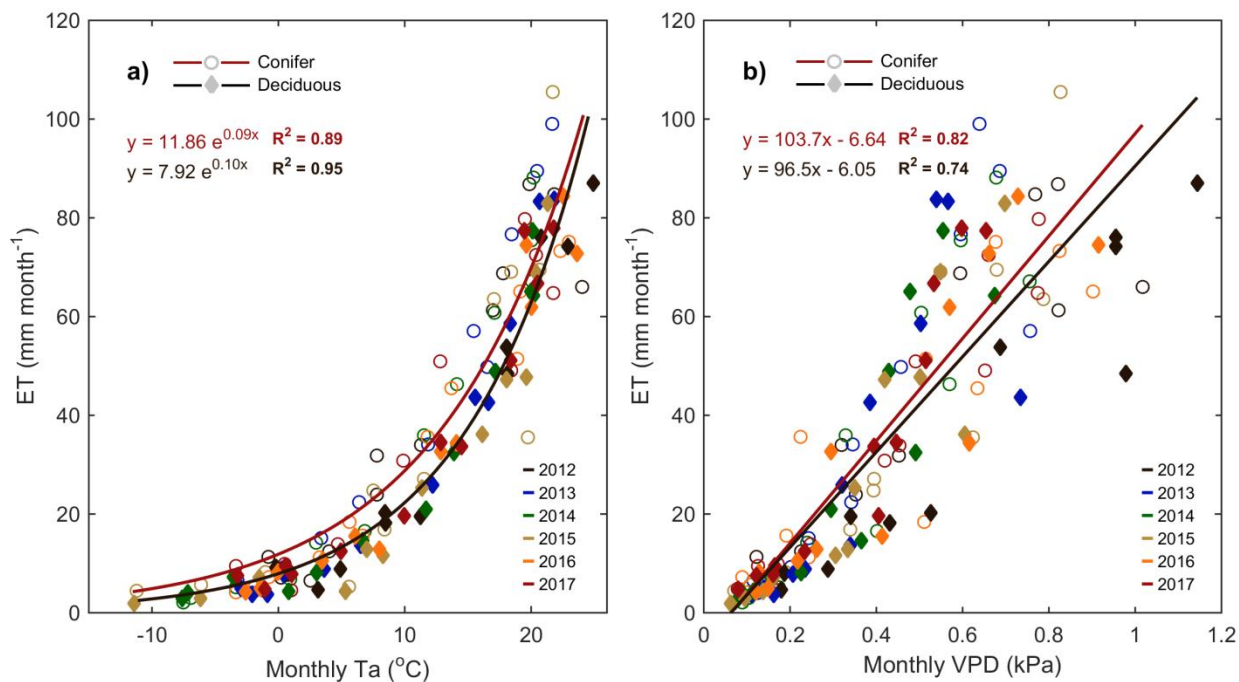


Figure 6. Annual smoothed (1-month moving average) time series of the (a) conifer (TP39) and (b) deciduous forest water use efficiency (WUE; GEP ET^{-1}), and (c) monthly linear relationships between GEP and ET at both sites from 2012 to 2017. Similarly, light use efficiency (LUE; GEP APAR^{-1}) calculations are shown for (d) the conifer forest and (e) deciduous forest, while linear relationships (f) of monthly GEP and APAR are also shown. Green shading corresponds to the site-specific 6-year mean phenological spring, while brown shading corresponds to the 6-year mean phenological autumn (Table 2). Linear fit equations and R² values are also shown (c & f).

1105

1110



1115 **Figure 7.** (a) Monthly exponential relationships between monthly mean air temperature (T_a) and total monthly evapotranspiration (ET) from 2012 to 2017 for the conifer (TP39, open circle) and deciduous (TPD, diamond) forests. Also shown are the six-year (b) linear relationships between monthly mean vapor pressure deficit (VPD) and monthly ET. Fit equations and R^2 also shown.

1120

1125



1130 **Table A1.** Descriptions of the eddy covariance (EC) instrumentation and meteorological sensors used at both sites during the period of measurements. *Note: IRGA = infrared gas analyzer*

	Turkey Point 1939 (TP39)	Turkey Point Deciduous (TPD)
Canopy IRGA	LI-7000 (LI-COR)	LI-7200 (LI-COR)
Sonic Anemometer	CSAT3 (CSI)	CSAT3 (CSI)
Height	28 m (2003 – May 2016) 34 m (May 2016 – Present)	36 m (2012 – Present)
Orientation	Oriented west (270°)	Oriented west (270°)
Intake Tube	4 m long intake tube	1 m long intake tube
Flow	15 L/min	15 L/min
Mid-Canopy IRGA	LI-800 (LI-COR) Measured at 14 m height	LI-820 (LI-COR) Measured at 16 m height
Air Temperature (Ta)	HMP45C (CSI)	HMP155A (CSI)
Relative Humidity (RH)		
Wind Speed & Direction	Model 05103 (R.M. Young)	Model 85000 (2012 – 2015) Model 05013 (2015 – Present)
Photosynthetically Active Radiation (PAR)	PAR-Lite (Kipp & Zonen)	PQSI (Kipp & Zonen)
Net Radiation (Rn)	CNR1 (Kipp & Zonen)	CNR4 (Kipp & Zonen)
Soil Temperature (Ts)	107B (CSI)	107B (CSI)
Soil Water Content (θ)	CS615-L/CS616 (CSI)	CS650 (CSI)
Precipitation (P)	T-200B (GEONOR)	CS700H-L (CSI)